Yukawa alignment revisited in the Higgs basis

Jae Sik Lee[1,2,*] and Jubin Park[2,†]

[1]*Department of Physics, Chonnam National University, Gwangju 61186, Korea*
[2]*IUEP, Chonnam National University, Gwangju 61186, Korea*

(Received 16 February 2022; accepted 11 July 2022; published 22 July 2022)

We implement a comprehensive and detailed study of the alignment of Yukawa couplings in the so-called Higgs basis taking the framework of general two Higgs doublet models (2HDMs). We clarify the model input parameters and derive the Yukawa couplings considering the two types of *CP*-violating sources: One from the Higgs potential and the other from the three complex alignment parameters $\zeta_{f=u,d,e}$. We consider the theoretical constraints from the perturbative unitarity and for the Higgs potential to be bounded from below as well as the experimental ones from electroweak precision observables. Also considered are the constraints on the alignment parameters from flavor-changing τ decays, $Z \to b\bar{b}$, ϵ_K, and the radiative $b \to s\gamma$ decay. By introducing the basis-independent Yukawa delay factor $\Delta_{H_1\bar{f}f} \equiv |\zeta_f|(1 - g^2_{H_1VV})^{1/2}$, we scrutinize the alignment of the Yukawa couplings of the lightest Higgs boson to the SM fermions.

DOI: 10.1103/PhysRevD.106.015023

I. INTRODUCTION

Since the discovery of the 125 GeV Higgs boson in 2012 at the LHC [1,2], it has been inspected very closely and extensively. At the early stage, several model-independent studies [3–25] show that there were some rooms for it to be unlike the one predicted in the Standard Model (SM), but, after combining all the LHC Higgs data at 7 and 8 TeV [26] and especially those at 13 TeV [27–45], it turns out that it is best described by the SM Higgs boson. Specifically, the third-generation Yukawa couplings have been established, and the most recent model-independent study [46] shows that the 1σ error of the top-quark Yukawa coupling is about 6% while those of the bottom-quark and tau-lepton ones are about 10%.[1] In addition, the possibility of negative top-quark Yukawa coupling has been completely ruled out and the bottom-quark Yukawa coupling shows a preference of the positive sign[2] at about 1.5σ level. For the tau-Yukawa coupling, the current data still do not show any preference for its sign yet. On the other hand, the coupling to a pair of massive vector bosons is constrained to be consistent with the SM value within about 5% at 1σ level.

Even though we have not seen any direct hint or evidence of new physics beyond the SM (BSM), we are eagerly anticipating it with various compelling motivations such as the tiny but nonvanishing neutrino masses, matter dominance of our Universe and its evolution driven by dark energy and dark matters, etc., [49]. In many BSM models, the Higgs sector is extended and it results in the existence of several neutral and charged Higgs bosons. Their distinctive features depending on new theoretical frameworks could be directly probed through their productions and decays at future high-energy and high-precision experiments [50–65].

By the alignment of the Yukawa couplings in general two Higgs doublet models (2HDMs) [66–75], first of all, we imply that the Yukawa matrices describing the couplings of the two Higgs doublets to the SM fermions should be aligned in the flavor space to avoid the tree-level Higgs-mediated flavor-changing neutral current (FCNC). In 2HDMs, there are three neutral Higgs bosons and one of them should be identified as the observed one at the LHC which weighs 125.5 GeV [76]. In this case, by the alignment of the Yukawa couplings, we also mean that the couplings of this SM-like Higgs boson to the SM fermions should be the same as those

*jslee@jnu.ac.kr
†honolov77@gmail.com

[1]Throughout this work, we are using the results presented in Ref. [46] which are based on global fits of the Higgs boson couplings to all the LHC Higgs data at 7 TeV, 8 TeV, and 13 TeV available up to the Summer 2018, corresponding to integrated luminosities per experiment of approximately 5/fb at 7 TeV, 20/fb at 8 TeV, and up to 80/fb at 13 TeV. We note that there are more datasets at 13 TeV up to 139/fb and 137/fb collected with the ATLAS and CMS experiments, respectively, see Refs. [47,48]. Though, without a combined ATLAS and CMS analysis, it is difficult to say conclusively how much the full 13-TeV dataset improves the measurements of Higgs boson properties quantitatively; we observe that the 1σ errors are reduced by the amount of about 30% by comparing the results presented in Ref. [47] with those in Ref. [45] in which the dataset up to 80/fb is used.

[2]Precisely speaking, here the sign of the bottom-quark Yukawa coupling is relative to the top-quark Yukawa coupling configured through the b- and t-quark loop contributions to the Hgg vertex.

of the SM Higgs boson itself or its couplings are strongly constrained to be very SM-like by the current LHC data as outlined above. One of the popular ways to achieve this alignment is to identify the lightest neutral Higgs boson as the 125.5 GeV one and assume that all the other Higgs bosons are heavier or much heavier than the lightest one [77,78]. But this decoupling scenario is not phenomenologically interesting and another scenario is suggested in which all the couplings of the SM-like Higgs candidate are (almost) aligned with those of the SM Higgs while the other Higgs bosons are not so heavy [79–82].

The alignment of Yukawa couplings are previously discussed and studied [80,83]. For some recent works, see, for example, Refs. [84–87]. In this work, taking the framework of general 2HDMs, we implement a comprehensive and detailed study of the alignment of Yukawa couplings in the so-called Higgs basis [73,74,88–92] in which only the doublet containing the SM-like Higgs boson develops the nonvanishing vacuum expectation value (vev) v. For the alignment of the Yukawa matrices, we assume that the Yukawa matrices are aligned in the flavor space [93–95] by introducing the three alignment parameters ζ_f with $f = u, d, e$ for the couplings to the up-type quarks, the down-type quarks, and the charged leptons, respectively. Under this assumption, there are no Higgs-mediated FCNC couplings at tree level and, at higher orders, they are very suppressed [94–98]. Then, we identify the lightest neutral Higgs boson as the 125.5 GeV one and consider the alignment of its Yukawa couplings as the masses of the heavier Higgs bosons increase or as the heavy Higgs bosons decouple. We figure that the decoupling of the Yukawa couplings of the lightest Higgs boson is delayed by the amount of $\Delta_{H_1\bar{f}f} \equiv |\zeta_f|(1 - g^2_{H_1VV})^{1/2}$ compared to its coupling to a pair of massive vector bosons, g_{H_1VV}. We observe that the Yukawa delay factor $\Delta_{H_1\bar{f}f}$ can be sizable even when $g_{H_1VV} \sim 1$ if $|\zeta_f|$ is significantly larger than 1. We consider the upper limit on $|\zeta_u|$ from $Z \to b\bar{b}$ and ϵ_K, and, for $|\zeta_d|$ and $|\zeta_e|$, we demonstrate that they are constrained to be small by the precision LHC Higgs data unless the so-called wrong-sign alignment of the Yukawa couplings [78,99–102] occurs.[3] Note that the Yukawa delay factor is basis-independent and can be used even when some of the Higgs potential parameters and/or all of the three alignment parameters are complex.

We emphasize that, we are reconsidering the decoupling behavior of the Yukawa couplings in the light of the new basis-independent measure of the Yukawa delay factor $\Delta_{H_1\bar{f}f}$ taking the aligned 2HDM in the Higgs basis. In the Higgs basis, contrasting to the relatively well-known Φ basis, it is easier to understand the analytic structure of intercorrelations among the model parameters. On the other hand, in the aligned 2HDM, there are three uncorrelated complex alignment parameters which provide further CP-violating sources in addition to those in the Higgs potential. The aligned 2HDM accommodates the conventional four types of 2HDMs as the limiting cases when the alignment parameters are real and fully correlated.

This paper is organized as follows. Section II is devoted to a brief review of the 2HDM Higgs potential, the mixing among neutral Higgs bosons and their couplings to the SM particles in the Higgs basis. In Sec. III, we elaborate on the constraints from the perturbative unitarity, the Higgs potential bounded from below, and the electroweak precision observables as well as the flavor constraints on the alignment parameters, and we carry out numerical analysis of the constraints and the alignment of Yukawa couplings in Sec. IV. A brief summary and conclusions are made in Sec. V.

II. TWO HIGGS DOUBLET MODEL IN THE HIGGS BASIS

In this section, we study the two Higgs doublet model taking the so-called Higgs basis [73,74,88–92]. We consider the general potential containing 3 dimensionful quadratic and 7 dimensionless quartic parameters, of which four parameters are complex. We closely examine the relations among the potential parameters, Higgs-boson masses, and the neutral Higgs-boson mixing so as to figure out the set of input parameters to be used in the next Section. We further work out the Yukawa couplings in the Higgs basis together with the interactions of the neutral and charged Higgs bosons with massive gauge bosons.

A. Higgs potential

The general 2HDM scalar potential containing two complex $\mathrm{SU}(2)_L$ doublets of Φ_1 and Φ_2 with the same hypercharge $Y = 1/2$ may be given by [65][4]

$$\begin{aligned} V_\Phi = {} & \mu_1^2(\Phi_1^\dagger\Phi_1) + \mu_2^2(\Phi_2^\dagger\Phi_2) + m_{12}^2(\Phi_1^\dagger\Phi_2) + m_{12}^{*2}(\Phi_2^\dagger\Phi_1) \\ & + \lambda_1(\Phi_1^\dagger\Phi_1)^2 + \lambda_2(\Phi_2^\dagger\Phi_2)^2 + \lambda_3(\Phi_1^\dagger\Phi_1)(\Phi_2^\dagger\Phi_2) + \lambda_4(\Phi_1^\dagger\Phi_2)(\Phi_2^\dagger\Phi_1) \\ & + \lambda_5(\Phi_1^\dagger\Phi_2)^2 + \lambda_5^*(\Phi_2^\dagger\Phi_1)^2 + \lambda_6(\Phi_1^\dagger\Phi_1)(\Phi_1^\dagger\Phi_2) + \lambda_6^*(\Phi_1^\dagger\Phi_1)(\Phi_2^\dagger\Phi_1) \\ & + \lambda_7(\Phi_2^\dagger\Phi_2)(\Phi_1^\dagger\Phi_2) + \lambda_7^*(\Phi_2^\dagger\Phi_2)(\Phi_2^\dagger\Phi_1), \end{aligned} \tag{1}$$

[3] In the wrong-sign alignment limit, the Yukawa couplings are equal in strength but opposite in sign to the SM ones.
[4] In contrast with the Higgs basis which has been taken for this work, we address it as the Φ basis.

in terms of 2 real and 1 complex dimensionful quadratic couplings and 4 real and 3 complex dimensionless quartic couplings. Note that the $\mathbf{Z}_2$ symmetry under $\Phi_1 \to \pm\Phi_1$ and $\Phi_2 \to \mp\Phi_2$ is hardly broken by the nonvanishing quartic couplings λ_6 and λ_7 and, in this case, we have three rephasing-invariant CP-violating phases in the potential. With the general parametrization of two scalar doublets $\Phi_{1,2}$ as

$$\Phi_1 = \begin{pmatrix} \phi_1^+ \\ \frac{1}{\sqrt{2}}(v_1 + \phi_1 + ia_1) \end{pmatrix}; \qquad \Phi_2 = e^{i\xi}\begin{pmatrix} \phi_2^+ \\ \frac{1}{\sqrt{2}}(v_2 + \phi_2 + ia_2) \end{pmatrix}, \tag{2}$$

and denoting $v_1 = v\cos\beta = vc_\beta$ and $v_2 = v\sin\beta = vs_\beta$ with $v = \sqrt{v_1^2 + v_2^2}$, one may remove μ_1^2, μ_2^2, and $\Im\mathrm{m}(m_{12}^2 e^{i\xi})$ from the 2HDM potential using three tadpole conditions:

$$\begin{aligned} \mu_1^2 &= -v^2\left[\lambda_1 c_\beta^2 + \frac{1}{2}\lambda_3 s_\beta^2 + c_\beta s_\beta \Re\mathrm{e}(\lambda_6 e^{i\xi})\right] + s_\beta^2 M_{H^\pm}^2, \\ \mu_2^2 &= -v^2\left[\lambda_2 s_\beta^2 + \frac{1}{2}\lambda_3 c_\beta^2 + c_\beta s_\beta \Re\mathrm{e}(\lambda_7 e^{i\xi})\right] + c_\beta^2 M_{H^\pm}^2, \\ \Im\mathrm{m}(m_{12}^2 e^{i\xi}) &= -\frac{v^2}{2}[2c_\beta s_\beta \Im\mathrm{m}(\lambda_5 e^{2i\xi}) + c_\beta^2 \Im\mathrm{m}(\lambda_6 e^{i\xi}) + s_\beta^2 \Im\mathrm{m}(\lambda_7 e^{i\xi})], \end{aligned} \tag{3}$$

with the square of the charged Higgs-boson mass

$$M_{H^\pm}^2 = -\frac{\Re\mathrm{e}(m_{12}^2 e^{i\xi})}{c_\beta s_\beta} - \frac{v^2}{2c_\beta s_\beta}[\lambda_4 c_\beta s_\beta + 2c_\beta s_\beta \Re\mathrm{e}(\lambda_5 e^{2i\xi}) + c_\beta^2 \Re\mathrm{e}(\lambda_6 e^{i\xi}) + s_\beta^2 \Re\mathrm{e}(\lambda_7 e^{i\xi})]. \tag{4}$$

On the other hand, in the Higgs basis where only one doublet contains the nonvanishing vev v, the general 2HDM scalar potential again contains three (two real and one complex) massive parameters and four real and three complex dimensionless quartic couplings and it might take the same form as in the Φ basis:

$$\begin{aligned} V_{\mathcal{H}} = {} & Y_1(\mathcal{H}_1^\dagger\mathcal{H}_1) + Y_2(\mathcal{H}_2^\dagger\mathcal{H}_2) + Y_3(\mathcal{H}_1^\dagger\mathcal{H}_2) + Y_3^*(\mathcal{H}_2^\dagger\mathcal{H}_1) \\ & + Z_1(\mathcal{H}_1^\dagger\mathcal{H}_1)^2 + Z_2(\mathcal{H}_2^\dagger\mathcal{H}_2)^2 + Z_3(\mathcal{H}_1^\dagger\mathcal{H}_1)(\mathcal{H}_2^\dagger\mathcal{H}_2) + Z_4(\mathcal{H}_1^\dagger\mathcal{H}_2)(\mathcal{H}_2^\dagger\mathcal{H}_1) \\ & + Z_5(\mathcal{H}_1^\dagger\mathcal{H}_2)^2 + Z_5^*(\mathcal{H}_2^\dagger\mathcal{H}_1)^2 + Z_6(\mathcal{H}_1^\dagger\mathcal{H}_1)(\mathcal{H}_1^\dagger\mathcal{H}_2) + Z_6^*(\mathcal{H}_1^\dagger\mathcal{H}_1)(\mathcal{H}_2^\dagger\mathcal{H}_1) \\ & + Z_7(\mathcal{H}_2^\dagger\mathcal{H}_2)(\mathcal{H}_1^\dagger\mathcal{H}_2) + Z_7^*(\mathcal{H}_2^\dagger\mathcal{H}_2)(\mathcal{H}_2^\dagger\mathcal{H}_1), \end{aligned} \tag{5}$$

where the new complex $\mathrm{SU}(2)_L$ doublets of $\mathcal{H}_1$ and $\mathcal{H}_2$ are given by the linear combinations of Φ_1 and Φ_2 as follows:

$$\begin{aligned} \mathcal{H}_1 &= c_\beta\Phi_1 + e^{-i\xi}s_\beta\Phi_2 = \begin{pmatrix} G^+ \\ \frac{1}{\sqrt{2}}(v + \varphi_1 + iG^0) \end{pmatrix}; \\ \mathcal{H}_2 &= -s_\beta\Phi_1 + e^{-i\xi}c_\beta\Phi_2 = \begin{pmatrix} H^+ \\ \frac{1}{\sqrt{2}}(\varphi_2 + ia) \end{pmatrix}, \end{aligned} \tag{6}$$

with the relations

$$\begin{aligned} &\varphi_1 \equiv c_\beta\phi_1 + s_\beta\phi_2, \qquad \varphi_2 \equiv -s_\beta\phi_1 + c_\beta\phi_2; \\ &a = -s_\beta a_1 + c_\beta a_2, \end{aligned} \tag{7}$$

in terms of $\phi_{1,2}$ and $a_{1,2}$ in Eq. (2). Incidentally, we have that $G^0 = c_\beta a_1 + s_\beta a_2$, $G^+ = c_\beta\phi_1^+ + s_\beta\phi_2^+$, and $H^+ = -s_\beta\phi_1^+ + c_\beta\phi_2^+$. Note that only the neutral component of the $\mathcal{H}_1$ doublet develops the nonvanishing vacuum expectation value v and it contains only one physical degree of freedom let alone the Goldstone modes. In the so-called decoupling limit, $\mathcal{H}_1$ takes over the role of the SM $\mathrm{SU}(2)_L$ doublet and the remaining three Higgs states are accommodated only by the $\mathcal{H}_2$ doublet.[5]

The potential parameters $Y_{1,2,3}$ and Z_{1-7} in the Higgs basis could be related to those in the Φ basis through:

$$\begin{aligned} Y_1 &= \mu_1^2 c_\beta^2 + \mu_2^2 s_\beta^2 + \Re\mathrm{e}(m_{12}^2 e^{i\xi})s_{2\beta}, \\ Y_2 &= \mu_1^2 s_\beta^2 + \mu_2^2 c_\beta^2 - \Re\mathrm{e}(m_{12}^2 e^{i\xi})s_{2\beta}, \\ Y_3 &= -(\mu_1^2 - \mu_2^2)c_\beta s_\beta + \Re\mathrm{e}(m_{12}^2 e^{i\xi})c_{2\beta} + i\Im\mathrm{m}(m_{12}^2 e^{i\xi}), \end{aligned} \tag{8}$$

for two real and one complex dimensionful parameters and[6]

[5]For a numerical study later, the notations of $\varphi_1 = h$, $\varphi_2 = H$, and $a = A$ are taken in the decoupling limit.

[6]We find that our results are consistent with those presented in, for example, Ref. [85].

$$
\begin{aligned}
Z_1 &= \lambda_1 c_\beta^4 + \lambda_2 s_\beta^4 + 2\lambda_{345} c_\beta^2 s_\beta^2 + [\mathrm{Re}(\lambda_6 e^{i\xi}) c_\beta^2 + \mathrm{Re}(\lambda_7 e^{i\xi}) s_\beta^2] s_{2\beta}, \\
Z_2 &= \lambda_1 s_\beta^4 + \lambda_2 c_\beta^4 + 2\lambda_{345} c_\beta^2 s_\beta^2 - [\mathrm{Re}(\lambda_6 e^{i\xi}) s_\beta^2 + \mathrm{Re}(\lambda_7 e^{i\xi}) c_\beta^2] s_{2\beta}, \\
Z_3 &= \lambda_3 + 2(\lambda_1 + \lambda_2 - 2\lambda_{345}) c_\beta^2 s_\beta^2 - [\mathrm{Re}(\lambda_6 e^{i\xi}) - \mathrm{Re}(\lambda_7 e^{i\xi})] c_{2\beta} s_{2\beta}, \\
Z_4 &= \lambda_4 + 2(\lambda_1 + \lambda_2 - 2\lambda_{345}) c_\beta^2 s_\beta^2 - [\mathrm{Re}(\lambda_6 e^{i\xi}) - \mathrm{Re}(\lambda_7 e^{i\xi})] c_{2\beta} s_{2\beta}, \\
Z_5 &= (\lambda_1 + \lambda_2 - 2\lambda_{345}) c_\beta^2 s_\beta^2 + \mathrm{Re}(\lambda_5 e^{2i\xi}) - [\mathrm{Re}(\lambda_6 e^{i\xi}) - \mathrm{Re}(\lambda_7 e^{i\xi})] c_{2\beta} c_\beta s_\beta \\
&\quad + i[\mathrm{Im}(\lambda_5 e^{2i\xi}) c_{2\beta} - \mathrm{Im}(\lambda_6 e^{i\xi}) c_\beta s_\beta + \mathrm{Im}(\lambda_7 e^{i\xi}) c_\beta s_\beta], \\
Z_6 &= (-\lambda_1 c_\beta^2 + \lambda_2 s_\beta^2) s_{2\beta} + 2\lambda_{345} c_{2\beta} c_\beta s_\beta + \mathrm{Re}(\lambda_6 e^{i\xi})(c_\beta^2 - 3 s_\beta^2) c_\beta^2 + \mathrm{Re}(\lambda_7 e^{i\xi})(3 c_\beta^2 - s_\beta^2) s_\beta^2 \\
&\quad + i[\mathrm{Im}(\lambda_5 e^{2i\xi}) s_{2\beta} + \mathrm{Im}(\lambda_6 e^{i\xi}) c_\beta^2 + \mathrm{Im}(\lambda_7 e^{i\xi}) s_\beta^2], \\
Z_7 &= (-\lambda_1 s_\beta^2 + \lambda_2 c_\beta^2) s_{2\beta} - 2\lambda_{345} c_{2\beta} c_\beta s_\beta + \mathrm{Re}(\lambda_6 e^{i\xi})(3 c_\beta^2 - s_\beta^2) s_\beta^2 + \mathrm{Re}(\lambda_7 e^{i\xi})(c_\beta^2 - 3 s_\beta^2) c_\beta^2 \\
&\quad + i[-\mathrm{Im}(\lambda_5 e^{2i\xi}) s_{2\beta} + \mathrm{Im}(\lambda_6 e^{i\xi}) s_\beta^2 + \mathrm{Im}(\lambda_7 e^{i\xi}) c_\beta^2],
\end{aligned} \tag{9}
$$

for four real and three complex dimensionless parameters with $\lambda_{345} \equiv (\lambda_3 + \lambda_4)/2 + \mathrm{Re}(\lambda_5 e^{2i\xi})$. We note that $Z_1 \leftrightarrow Z_2$, $Z_3 \leftrightarrow Z_4$, $Z_6 \leftrightarrow Z_7$, and Z_5 are invariant under the exchanges $c_\beta \leftrightarrow s_\beta$, $\lambda_3 \leftrightarrow \lambda_4$, $(\lambda_5 e^{2i\xi}) \leftrightarrow (\lambda_5 e^{2i\xi})^*$, $(\lambda_{6,7} e^{i\xi}) \leftrightarrow -(\lambda_{6,7} e^{i\xi})^*$. The tadpole conditions in the Higgs basis, which are much simpler than those in the Φ basis, as shown in Eq. (3), are

$$
Y_1 + Z_1 v^2 = 0; \qquad Y_3 + \frac{1}{2} Z_6 v^2 = 0, \tag{10}
$$

where the first condition comes from $\langle \frac{\partial V_{\mathcal{H}}}{\partial \varphi_1} \rangle = 0$ and the second one from $\langle \frac{\partial V_{\mathcal{H}}}{\partial \varphi_2} \rangle = 0$ and $\langle \frac{\partial V_{\mathcal{H}}}{\partial a} \rangle = 0$. Note that the second condition relates the two complex parameters of Y_3 and Z_6.

B. Masses, mixing, and potential parameters in the Higgs basis

In the Higgs basis, the 2HDM Higgs potential includes the mass terms which can be cast into the form consisting of two parts

$$
V_{\mathcal{H},\mathrm{mass}} = M_{H^\pm}^2 H^+ H^- + \frac{1}{2} (\varphi_1 \;\; \varphi_2 \;\; a) \mathcal{M}_0^2 \begin{pmatrix} \varphi_1 \\ \varphi_2 \\ a \end{pmatrix}, \tag{11}
$$

in terms of the charged Higgs bosons $H^\pm$, two neutral scalars $\varphi_{1,2}$, and one neutral pseudoscalar a. The charged Higgs boson mass is given by

$$
M_{H^\pm}^2 = Y_2 + \frac{1}{2} Z_3 v^2, \tag{12}
$$

while the 3×3 mass-squared matrix of the neutral Higgs bosons $\mathcal{M}_0^2$ takes the form

$$
\mathcal{M}_0^2 = M_A^2 \mathrm{diag}(0, 1, 1) + \mathcal{M}_Z^2, \tag{13}
$$

where $M_A^2 = M_{H^\pm}^2 + [\frac{1}{2} Z_4 - \mathrm{Re}(Z_5)] v^2$ and the 3×3 real and symmetric mass-squared matrix $\mathcal{M}_Z^2$ is given by

$$
\frac{\mathcal{M}_Z^2}{v^2} = \begin{pmatrix} 2Z_1 & \mathrm{Re}(Z_6) & -\mathrm{Im}(Z_6) \\ \mathrm{Re}(Z_6) & 2\mathrm{Re}(Z_5) & -\mathrm{Im}(Z_5) \\ -\mathrm{Im}(Z_6) & -\mathrm{Im}(Z_5) & 0 \end{pmatrix}. \tag{14}
$$

Note that the quartic couplings Z_2 and Z_7 have nothing to do with the masses of Higgs bosons and the mixing of the neutral ones. They can be probed only through the cubic and quartic Higgs self-couplings, see Eq. (5) while noting that only the $\mathcal{H}_1$ doublet contains the vev $v \simeq 246$ GeV. We further note that φ_1 decouples from the mixing with the other two neutral states of φ_2 and a in the $Z_6 = 0$ limit, and its mass squared is simply given by $2Z_1 v^2$ which gives $Z_1 \simeq 0.13 (M_{H_1}/125.5\ \mathrm{GeV})^2$, and, in this decoupling limit of $Z_6 \to 0$, the CP-violating mixing between the two states of φ_2 and a is dictated only by $\mathrm{Im}(Z_5)$.

Once the 3×3 real and symmetric mass-squared matrix $\mathcal{M}_0^2$ is given, the orthogonal 3×3 mixing matrix O is defined through[7]

$$
(\varphi_1, \varphi_2, a)_\alpha^T = O_{\alpha i} (H_1, H_2, H_3)_i^T, \tag{15}
$$

such that $O^T \mathcal{M}_0^2 O = \mathrm{diag}(M_{H_1}^2, M_{H_2}^2, M_{H_3}^2)$ with the increasing ordering of $M_{H_1} \le M_{H_2} \le M_{H_3}$, if necessary. Note that the mass-squared matrix $\mathcal{M}_0^2$ involves only the four (two real and two complex) quartic couplings

[7]Note that, we reserve the notations of $H_{i=1,2,3}$ for the mass eigenstates of three neutral Higgs bosons taking account of CP-violating mixing in the neutral Higgs-boson sector when $\mathrm{Im}(Z_{5,6}) \neq 0$. In general, the neutral Higgs bosons do not carry definite CP parities and they become mixtures of CP-even and CP-odd states.

$\{Z_1, Z_4, Z_5, Z_6\}$ once v and $M_{H^\pm}$ are given. And then, using the matrix relation $O^T\mathcal{M}_0^2 O = \mathrm{diag}(M_{H_1}^2, M_{H_2}^2, M_{H_3}^2)$, one may find the following expressions for the quartic couplings of $\{Z_1, Z_4, Z_5, Z_6\}$ in terms of the three masses of neutral Higgs bosons and the components of the 3×3 orthogonal mixing matrix O[8]:

$$\begin{aligned}
Z_1 &= \frac{1}{2v^2}(M_{H_1}^2 O_{\varphi_1 1}^2 + M_{H_2}^2 O_{\varphi_1 2}^2 + M_{H_3}^2 O_{\varphi_1 3}^2),\\
Z_4 &= \frac{1}{v^2}[M_{H_1}^2(O_{\varphi_2 1}^2 + O_{a1}^2) + M_{H_2}^2(O_{\varphi_2 2}^2 + O_{a2}^2)\\
&\quad + M_{H_3}^2(O_{\varphi_2 3}^2 + O_{a3}^2) - 2M_{H^\pm}^2],\\
Z_5 &= \frac{1}{2v^2}[M_{H_1}^2(O_{\varphi_2 1}^2 - O_{a1}^2) + M_{H_2}^2(O_{\varphi_2 2}^2 - O_{a2}^2)\\
&\quad + M_{H_3}^2(O_{\varphi_2 3}^2 - O_{a3}^2)]\\
&\quad - \frac{i}{v^2}(M_{H_1}^2 O_{\varphi_2 1}O_{a1} + M_{H_2}^2 O_{\varphi_2 2}O_{a2} + M_{H_3}^2 O_{\varphi_2 3}O_{a3}),\\
Z_6 &= \frac{1}{v^2}(M_{H_1}^2 O_{\varphi_1 1}O_{\varphi_2 1} + M_{H_2}^2 O_{\varphi_1 2}O_{\varphi_2 2} + M_{H_3}^2 O_{\varphi_1 3}O_{\varphi_2 3})\\
&\quad - \frac{i}{v^2}(M_{H_1}^2 O_{\varphi_1 1}O_{a1} + M_{H_2}^2 O_{\varphi_1 2}O_{a2} + M_{H_3}^2 O_{\varphi_1 3}O_{a3}),
\end{aligned} \tag{16}$$

for given v and $M_{H^\pm}$.

Now we are ready to consider the input parameters for 2HDM in the Higgs basis. First of all, the input parameters for the Higgs potential Eq. (5) are

$$\{Y_1, Y_2, Y_3; Z_1, Z_2, Z_3, Z_4, Z_5, Z_6, Z_7\}. \tag{17}$$

Using the tadpole conditions in Eq. (10), the dimensionful parameters Y_1 and Y_3 can be removed from the set in favor of v and observing that the quartic couplings Z_2 and Z_7 do not contribute to the mass terms, one may consider the following set of input parameters:

$$\{v, Y_2; M_{H^\pm}, Z_1, Z_4, Z_5, Z_6; Z_2, Z_7\}, \tag{18}$$

where we trade the quartic coupling Z_3 with the charged Higgs mass $M_{H^\pm}$ using the relation $Z_3 = 2(M_{H^\pm}^2 - Y_2)/v^2$ with Y_2 given. Further using M_{H_i} and O instead of $\{Z_1, Z_4, Z_5, Z_6\}$, we end up with the following set of input parameters:

$$\mathcal{I} = \{v, Y_2; M_{H^\pm}, M_{H_1}, M_{H_2}, M_{H_3}, \{O_{3\times 3}\}; Z_2, Z_7\}, \tag{19}$$

which contains 12 real degrees of freedom. If desirable, one may remove the unphysical massive parameter Y_2 in favor of the dimensionless quartic coupling Z_3 by having an alternative set

$$\mathcal{I}' = \{v; M_{H^\pm}, M_{H_1}, M_{H_2}, M_{H_3}, \{O_{3\times 3}\}; Z_3; Z_2, Z_7\}, \tag{20}$$

consisting of 12 real parameters as well.

For example, in the CP-conserving (CPC) case with $\Im\mathrm{m}Z_5 = \Im\mathrm{m}Z_6 = 0$, one may denote the masses of the three neutral Higgs bosons by M_h, M_H, and M_A or $O^T\mathcal{M}_0^2 O = \mathrm{diag}(M_h^2, M_H^2, M_A^2)$. Note that $M_h^2 = 2Z_1 v^2$ is for the SM Higgs boson in the decoupling limit of $Z_6 \to 0$. The mixing matrix O can be parametrized as

$$O_{\mathrm{CPC}} = \begin{pmatrix} c_\gamma & s_\gamma & 0\\ -s_\gamma & c_\gamma & 0\\ 0 & 0 & 1\end{pmatrix}, \tag{21}$$

introducing the mixing angle γ between the two CP-even states φ_1 and φ_2. In this CP-conserving case, the relations Eq. (16) simplify into

$$\begin{aligned}
Z_1 &= \frac{1}{2v^2}(c_\gamma^2 M_h^2 + s_\gamma^2 M_H^2),\\
Z_4 &= \frac{1}{v^2}(s_\gamma^2 M_h^2 + c_\gamma^2 M_H^2 + M_A^2 - 2M_{H^\pm}^2),\\
Z_5 &= \frac{1}{2v^2}(s_\gamma^2 M_h^2 + c_\gamma^2 M_H^2 - M_A^2),\\
Z_6 &= \frac{1}{v^2}(-M_h^2 + M_H^2)c_\gamma s_\gamma.
\end{aligned} \tag{22}$$

We observe that, in the decoupling limit of $\sin\gamma = 0$, $Z_1 = M_h^2/2v^2$ and $Z_6 = 0$, and Z_4 and Z_5 are determined by the mass differences of $M_H^2 + M_A^2 - 2M_{H^\pm}^2$ and $M_H^2 - M_A^2$, respectively. Finally, for the study of the CPC case, one may choose one of the following two equivalent sets:

$$\begin{aligned}
\mathcal{I}_{\mathrm{CPC}} &= \{v, Y_2; M_{H^\pm}, M_h, M_H, M_A, \gamma; Z_2, Z_7\},\\
\mathcal{I}'_{\mathrm{CPC}} &= \{v; M_{H^\pm}, M_h, M_H, M_A, \gamma; Z_3; Z_2, Z_7\},
\end{aligned} \tag{23}$$

each of which contains 9 real degrees of freedom, and the convention of $|\gamma| \le \pi/2$ without loss of generality resulting in $c_\gamma \ge 0$ and $\mathrm{sign}(s_\gamma) = \mathrm{sign}(Z_6)$ if $M_H > M_h$ GeV.

In the presence of nonvanishing $\Im\mathrm{m}Z_5$ and/or $\Im\mathrm{m}Z_6$, the mixing between the two CP-even states $\varphi_{1,2}$ and the CP-odd one a arises leading to CP violation in the neutral Higgs sector. By introducing a rotation $\mathcal{H}_2 \to e^{i\zeta}\mathcal{H}_2$,[9] we note that the Higgs potential given by Eq. (5) is invariant under the following phase rotations:

$$\begin{aligned}
&\mathcal{H}_2 \to e^{+i\zeta}\mathcal{H}_2; \qquad Y_3 \to Y_3 e^{-i\zeta}, \qquad Z_5 \to Z_5 e^{-2i\zeta},\\
&Z_6 \to Z_6 e^{-i\zeta}, \qquad Z_7 \to Z_7 e^{-i\zeta}.
\end{aligned} \tag{24}$$

Considering the tadpole conditions Eq. (10), this might imply that one of the CP phases of $\Im\mathrm{m}(Z_5)$, $\Im\mathrm{m}(Z_6)$, and

[8]The 3×3 orthogonal mixing matrix O contains three independent degrees of freedom represented by the three rotation angles.

[9]Or, equivalently, $\mathcal{H}_1^\dagger\mathcal{H}_2 \to e^{i\zeta}\mathcal{H}_1^\dagger\mathcal{H}_2$.

$\Im\mathrm{m}(Z_7)$ can be rotated away by rephasing the Higgs fields $\mathcal{H}_2$. By keeping $\Im\mathrm{m}(Z_7)$ as an independent input and taking either $\Im\mathrm{m}(Z_5)=0$ or $\Im\mathrm{m}(Z_6)=0$, one may use the following set of input parameters[10]:

$$\mathcal{I}_{\mathrm{CPV}}=\{v,Y_2;M_{H^\pm},M_{H_1},M_{H_2},M_{H_3},\gamma,\{\omega\,\mathrm{or}\,\eta\};\\ Z_2,\Re\mathrm{e}(Z_7),\Im\mathrm{m}(Z_7)\},\tag{25}$$

which contains 11 real degrees of freedom. In this case, the mixing angle η (ω) can be fixed by solving $\Im\mathrm{m}(Z_5)=0$ or $\Im\mathrm{m}(Z_6)=0$ when $M_{H_{1,2,3}}$ and ω (η) are given. More explicitly, using the relations in Eq. (16), we have

$$\begin{aligned}\Im\mathrm{m}(Z_5)&=\left[\frac{M_{H_3}^2c_\omega^2+M_{H_2}^2s_\omega^2-M_{H_1}^2}{v^2}s_\gamma s_\eta\right.\\&\quad\left.-\frac{M_{H_3}^2-M_{H_2}^2}{v^2}c_\gamma c_\omega s_\omega\right]c_\eta\\&=\left[\frac{M_{H_3}^2+M_{H_2}^2-2M_{H_1}^2}{2v^2}s_\gamma s_\eta+\frac{M_{H_3}^2-M_{H_2}^2}{2v^2}s_\gamma s_\eta c_{2\omega}\right.\\&\quad\left.-\frac{M_{H_3}^2-M_{H_2}^2}{2v^2}c_\gamma s_{2\omega}\right]c_\eta\\\Im\mathrm{m}(Z_6)&=-\left[\frac{M_{H_3}^2c_\omega^2+M_{H_2}^2s_\omega^2-M_{H_1}^2}{v^2}c_\gamma s_\eta\right.\\&\quad\left.+\frac{M_{H_3}^2-M_{H_2}^2}{v^2}s_\gamma c_\omega s_\omega\right]c_\eta\\&=-\left[\frac{M_{H_3}^2+M_{H_2}^2-2M_{H_1}^2}{2v^2}c_\gamma s_\eta+\frac{M_{H_3}^2-M_{H_2}^2}{2v^2}c_\gamma s_\eta c_{2\omega}\right.\\&\quad\left.+\frac{M_{H_3}^2-M_{H_2}^2}{2v^2}s_\gamma s_{2\omega}\right]c_\eta,\end{aligned}\tag{26}$$

parametrizing the mixing matrix O as follows:

$$\begin{aligned}O_{\mathrm{CPV}}&=O_\gamma O_\eta O_\omega\\&\equiv\begin{pmatrix}c_\gamma&s_\gamma&0\\-s_\gamma&c_\gamma&0\\0&0&1\end{pmatrix}\begin{pmatrix}c_\eta&0&s_\eta\\0&1&0\\-s_\eta&0&c_\eta\end{pmatrix}\begin{pmatrix}1&0&0\\0&c_\omega&s_\omega\\0&-s_\omega&c_\omega\end{pmatrix}\\&=\begin{pmatrix}c_\gamma c_\eta&s_\gamma c_\omega-c_\gamma s_\eta s_\omega&s_\gamma s_\omega+c_\gamma s_\eta c_\omega\\-s_\gamma c_\eta&c_\gamma c_\omega+s_\gamma s_\eta s_\omega&c_\gamma s_\omega-s_\gamma s_\eta c_\omega\\-s_\eta&-c_\eta s_\omega&c_\eta c_\omega\end{pmatrix}.\end{aligned}\tag{27}$$

Assuming $c_\eta\neq 0$ and, for example, taking γ and ω as the input mixing angles, the remaining mixing angle η is determined by

$$s_\eta|_{\Im\mathrm{m}Z_5=0}=\frac{(M_{H_3}^2-M_{H_2}^2)c_\gamma c_\omega s_\omega}{(M_{H_3}^2c_\omega^2+M_{H_2}^2s_\omega^2-M_{H_1}^2)s_\gamma},\tag{28}$$

imposing $\Im\mathrm{m}Z_5=0$. If $\Im\mathrm{m}Z_6=0$ is imposed instead, η is determined by

$$s_\eta|_{\Im\mathrm{m}Z_6=0}=-\frac{(M_{H_3}^2-M_{H_2}^2)s_\gamma c_\omega s_\omega}{(M_{H_3}^2c_\omega^2+M_{H_2}^2s_\omega^2-M_{H_1}^2)c_\gamma}.\tag{29}$$

Of course, using Z_3 instead of Y_2, one may use the alternative set

$$\mathcal{I}'_{\mathrm{CPV}}=\{v;M_{H^\pm},M_{H_1},M_{H_2},M_{H_3},\gamma,\{\omega\,\mathrm{or}\,\eta\};\\ Z_3;Z_2,\Re\mathrm{e}(Z_7),\Im\mathrm{m}(Z_7)\}.\tag{30}$$

Incidentally, one may choose the basis in which $\Im\mathrm{m}(Z_7)=0$ by taking the following set of input parameters:

$$\mathcal{I}''_{\mathrm{CPV}}=\{v;M_{H^\pm},M_{H_1},M_{H_2},M_{H_3},\gamma,\eta,\omega;Z_3;Z_2,Z_7\},\tag{31}$$

where all the three mixing angles are independent from one another and Z_7 is real.

In passing, we note that, in the limit of $c_\gamma=1$ and $s_\gamma=0$, the mixing matrix takes the simpler form

$$O_{\mathrm{CPV}}|_{\sin\gamma=0}=O_\eta O_\omega=\begin{pmatrix}c_\eta&-s_\eta s_\omega&s_\eta c_\omega\\0&c_\omega&s_\omega\\-s_\eta&-c_\eta s_\omega&c_\eta c_\omega\end{pmatrix}.\tag{32}$$

When $c_\eta\simeq 1-\eta^2/2$ and $s_\eta\simeq\eta$, the lightest H_1 is SM-like and the heavier ones $H_{2,3}$ are mostly arbitrary mixtures of φ_2 and a. On the other hand, when $c_\eta\simeq|\eta|$ and $|s_\eta|\simeq 1-\eta^2/2$, the lightest H_1 is mostly CP-odd ($H_1\sim a$) and H_2 (H_3) is SM-like when $|s_\omega|\simeq 1$ ($|c_\omega|\simeq 1$).

C. Yukawa couplings in Higgs basis

In the 2HDM, the Yukawa couplings might be given by [94]

$$-\mathcal{L}_Y=\sum_{k=1,2}\overline{Q_L^0}\,\mathbf{y}_k^u\tilde{\mathcal{H}}_k u_R^0+\overline{Q_L^0}\mathbf{y}_k^d\mathcal{H}_k d_R^0+\overline{L_L^0}\mathbf{y}_k^e\mathcal{H}_k e_R^0\\ +\mathrm{H.c.},\tag{33}$$

in terms of the six 3×3 Yukawa matrices $\mathbf{y}_{1,2}^{u,d,e}$ with the electroweak eigenstates $Q_L^0=(u_L^0,d_L^0)^T$, $L_L^0=(\nu_L^0,e_L^0)^T$, u_R^0, d_R^0, and e_R^0. The two Higgs doublets $\mathcal{H}_{1,2}$ in the Higgs basis are given by Eq. (6):

[10]In this CP-violating (CPV) case, we parametrize the mixing matrix O by introducing the three mixing angles of γ, η, and ω as explicitly shown in Eq. (27).

$$\mathcal{H}_1 = \left(G^+, \frac{1}{\sqrt{2}}(v+\varphi_1+iG^0)\right)^T,$$
$$\mathcal{H}_2 = \left(H^+, \frac{1}{\sqrt{2}}(\varphi_2+ia)\right)^T, \tag{34}$$

and their SU(2)-conjugated doublets by

$$\tilde{\mathcal{H}}_1 = i\tau_2\mathcal{H}_1^* = \left(\frac{1}{\sqrt{2}}(v+\varphi_1-iG^0), -G^-\right)^T,$$
$$\tilde{\mathcal{H}}_2 = i\tau_2\mathcal{H}_2^* = \left(\frac{1}{\sqrt{2}}(\varphi_2-ia), -H^-\right)^T. \tag{35}$$

The Yukawa interactions include the following mass terms:

$$-\mathcal{L}_{Y,\text{mass}} = \frac{v}{\sqrt{2}}(\overline{u_L^0}\mathbf{y}_1^u u_R^0 + \overline{d_L^0}\mathbf{y}_1^d d_R^0 + \overline{e_L^0}\mathbf{y}_1^e e_R^0 + \text{H.c.}), \tag{36}$$

which involve only the Yukawa matrices of $\mathbf{y}_1^{u,d,e}$. Therefore, introducing two unitary matrices relating the left/right-handed electroweak eigenstates $f_{L,R}^0$ to the left/right-handed mass eigenstates $f_{L,R}$ with $f = u,\ d,\ e$ as follows:

$$u_L^0 = \mathcal{U}_{u_L}u_L, \quad d_L^0 = \mathcal{U}_{d_L}d_L, \quad e_L^0 = \mathcal{U}_{e_L}e_L;$$
$$u_R^0 = \mathcal{U}_{u_R}u_R, \quad d_R^0 = \mathcal{U}_{d_R}d_R, \quad e_R^0 = \mathcal{U}_{e_R}e_R, \tag{37}$$

we have, for the mass terms,

$$-\mathcal{L}_{Y,\text{mass}} = \overline{u_L}\mathbf{M}_u u_R + \overline{d_L}\mathbf{M}_d d_R + \overline{e_L}\mathbf{M}_e e_R + \text{H.c.}, \tag{38}$$

where the three diagonal matrices are

$$\mathbf{M}_u = \frac{v}{\sqrt{2}}\mathcal{U}_{u_L}^\dagger \mathbf{y}_1^u \mathcal{U}_{u_R} = \text{diag}(m_u, m_c, m_t),$$
$$\mathbf{M}_d = \frac{v}{\sqrt{2}}\mathcal{U}_{d_L}^\dagger \mathbf{y}_1^d \mathcal{U}_{d_R} = \text{diag}(m_d, m_s, m_b),$$
$$\mathbf{M}_e = \frac{v}{\sqrt{2}}\mathcal{U}_{e_L}^\dagger \mathbf{y}_1^e \mathcal{U}_{e_R} = \text{diag}(m_e, m_\mu, m_\tau), \tag{39}$$

in terms of the six quark and three charged-lepton masses. We note that $\mathcal{U}_{u_L}^\dagger \mathcal{U}_{d_L} = V_{\text{CKM}} \equiv V$ is nothing but the CKM matrix and, by the use of it, the $\text{SU}(2)_L$ quark doublets in the electroweak basis can be related to those in the mass basis in the following two ways:

$$Q_L^0 = \mathcal{U}_{u_L}\begin{pmatrix} u_L \\ Vd_L \end{pmatrix} \quad \text{or} \quad Q_L^0 = \mathcal{U}_{d_L}\begin{pmatrix} V^\dagger u_L \\ d_L \end{pmatrix}. \tag{40}$$

The first relation is used for the Yukawa interactions with the right-handed up-type quarks and the second one for those with the right-handed down-type quarks. Incidentally, we also have

$$L_L^0 = \mathcal{U}_{e_L}\begin{pmatrix} \nu_L \\ e_L \end{pmatrix} \tag{41}$$

by defining $\nu_L \equiv \mathcal{U}_{e_L}^\dagger \nu_L^0$ with no physical effects in the case with vanishing neutrino masses.

Collecting all the parametrizations, unitary rotations, and reparametrizations, the couplings of the neutral Higgs bosons to two fermions are given by

$$-\mathcal{L}_{H\bar{f}f} = \frac{1}{v}[\bar{u}\mathbf{M}_u u]\varphi_1 + [\bar{u}(\mathbf{h}_u^H + \mathbf{h}_u^A\gamma_5)u]\varphi_2 + [\bar{u}(-i\mathbf{h}_u^A - i\mathbf{h}_u^H\gamma_5)u]a + \frac{1}{v}[\bar{d}\mathbf{M}_d d]\varphi_1 + [\bar{d}(\mathbf{h}_d^H + \mathbf{h}_d^A\gamma_5)d]\varphi_2$$
$$+ [\bar{d}(i\mathbf{h}_d^A + i\mathbf{h}_d^H\gamma_5)d]a + \frac{1}{v}[\bar{e}\mathbf{M}_e e]\varphi_1 + [\bar{e}(\mathbf{h}_e^H + \mathbf{h}_e^A\gamma_5)e]\varphi_2 + [\bar{e}(i\mathbf{h}_e^A + i\mathbf{h}_e^H\gamma_5)e]a, \tag{42}$$

where three Hermitian and three anti-Hermitian Yukawa coupling matrices are

$$\mathbf{h}_f^H \equiv \frac{\mathbf{h}_f + \mathbf{h}_f^\dagger}{2}, \qquad \mathbf{h}_f^A \equiv \frac{\mathbf{h}_f - \mathbf{h}_f^\dagger}{2}, \tag{43}$$

with $\mathbf{h}_{f=u,d,e}$ given in terms of the 3×3 Yukawa matrix $\mathbf{y}_2^f$ and two unitary matrices as

$$\mathbf{h}_f \equiv \frac{1}{\sqrt{2}}\mathcal{U}_{f_L}^\dagger \mathbf{y}_2^f \mathcal{U}_{f_R}. \tag{44}$$

We observe that the couplings of the φ_1 field are diagonal in the flavor space and their sizes are directly proportional to the masses of the fermions to which it couples. In contrast, those of the φ_2 and a fields are not diagonal in the flavor space leading to the tree-level Higgs-mediated FCNC and their magnitudes are arbitrary in principle.

To avoid the tree-level FCNC, the matrices $\mathbf{h}_{f=u,d,e}$ are desired to be diagonal which can be achieved by requiring [94][11]

[11]Under this requirement, the Yukawa matrix $\mathbf{h}_f$ for the Higgs field $\mathcal{H}_2$ is indeed diagonal with its diagonal components being proportional to the hierarchical fermion masses multiplied by the common factor ζ_f, see Eq. (46). For an alternative Yukawa alignment in which $\mathcal{H}_2$ can couple to light fermions sizably while still achieving the absence of tree-level FCNCs, see Ref. [103].

$$\mathbf{y}_2^f = \zeta_f \mathbf{y}_1^f, \tag{45}$$

along with introducing the three complex alignment parameters $\zeta_{f=u,d,e}$. In this case, the two aligned Yukawa matrices $\mathbf{y}_1^f$ and $\mathbf{y}_2^f$ can be diagonalized simultaneously and the Yukawa matrices describing the couplings of φ_2 and a fields to the fermion mass eigenstates are given by

$$\mathbf{h}_f = \zeta_f \frac{\mathbf{M}_f}{v}, \tag{46}$$

which leads to the Hermitian and anti-Hermitian Yukawa matrices

$$\mathbf{h}_f^H = \Re\mathrm{e}(\zeta_f)\frac{\mathbf{M}_f}{v}, \qquad \mathbf{h}_f^A = i\Im\mathrm{m}(\zeta_f)\frac{\mathbf{M}_f}{v}. \tag{47}$$

When $\Im\mathrm{m}(\zeta_f) = 0$, the conventional 2HDMs based on the Glashow-Weinberg condition [104] can be obtained by choosing ζ_f as shown in Table I. Otherwise, the couplings of the mass eigenstates of the neutral Higgs bosons $H_{i=1,2,3}$ to two fermions are given by

$$-\mathcal{L}_{H_i\bar{f}f} = \sum_{i=1}^{3}\sum_{f=u,d,c,s,t,b,e,\mu,\tau} \frac{m_f}{v}\bar{f}(g^S_{H_i\bar{f}f} + ig^P_{H_i\bar{f}f}\gamma_5)fH_i \tag{48}$$

with the scalar and pseudoscalar couplings given by

$$\begin{aligned} g^S_{H_i\bar{f}f} &= O_{\varphi_1 i} + \Re\mathrm{e}(\zeta_f)O_{\varphi_2 i} \pm \Im\mathrm{m}(\zeta_f)O_{ai}, \\ g^P_{H_i\bar{f}f} &= \Im\mathrm{m}(\zeta_f)O_{\varphi_2 i} \mp \Re\mathrm{e}(\zeta_f)O_{ai}, \end{aligned} \tag{49}$$

where the upper and lower signs are for the up-type fermions $f = u,\ c,\ t$ and the down-type fermions $f = d, s, b, e, \mu, \tau$, respectively. The simultaneous existence of the scalar $g^S_{H_i\bar{f}f}$ and pseudoscalar $g^P_{H_i\bar{f}f}$ couplings for a specific H_i signals the CP violation in the neutral Higgs sector. We figure out that there are two different sources of the neutral Higgs-sector CP violation: (i) one is the CP-violating mixing among the CP-even and CP-odd states arising in the presence of nonvanishing $\Im\mathrm{m}(Z_{5,6})$ in the Higgs potential and (ii) the other one is the complex alignment parameters of ζ_f's. Note that the second source is absent in the conventional four types of 2HDMs since ζ_f's are real in those models.

The couplings of charged Higgs bosons to two fermions are given by

$$\begin{aligned} -\mathcal{L}_{H^\pm\bar{f}_\uparrow f_\downarrow} &= -\sqrt{2}[\overline{u_R}(\mathbf{h}_u^\dagger V)d_L]H^+ + \sqrt{2}[\overline{u_L}(V\mathbf{h}_d)d_R]H^+ \\ &\quad + \sqrt{2}[\overline{\nu_L}\mathbf{h}_e e_R]H^+ + \mathrm{H.c.}, \end{aligned} \tag{50}$$

in terms of the CKM matrix V and the 3×3 Yukawa matrices $\mathbf{h}_{u,d,e}$.

Previously, we note that the Higgs potential given by Eq. (5) is invariant under the phase rotation $\mathcal{H}_2 \to \mathrm{e}^{i\zeta}\mathcal{H}_2$ if the complex potential parameters are accordingly rephased, see Eq. (24). This observation extends to the Yukawa interactions, Eq. (33), by noting that they are invariant under the phase rotations:

$$\begin{aligned} &\mathcal{H}_2 \to \mathrm{e}^{+i\zeta}\mathcal{H}_2; \qquad \mathbf{y}_2^u \to \mathrm{e}^{+i\zeta}\mathbf{y}_2^u, \\ &\mathbf{y}_2^d \to \mathrm{e}^{-i\zeta}\mathbf{y}_2^d, \qquad \mathbf{y}_2^e \to \mathrm{e}^{-i\zeta}\mathbf{y}_2^e. \end{aligned} \tag{51}$$

Under the alignment assumption $\mathbf{y}_2^f = \zeta_f\mathbf{y}_1^f$ given by Eq. (45), the above rephasing invariant rotations become

$$\begin{aligned} &\mathcal{H}_2 \to \mathrm{e}^{+i\zeta}\mathcal{H}_2; \qquad \zeta_u \to \mathrm{e}^{+i\zeta}\zeta_u, \\ &\zeta_d \to \mathrm{e}^{-i\zeta}\zeta_d, \qquad \zeta_e \to \mathrm{e}^{-i\zeta}\zeta_e, \end{aligned} \tag{52}$$

in terms of the complex alignment parameters. Then one may be able to show that the scalar and pseudoscalar couplings given by Eq. (49) are invariant under the phase rotations given by Eq. (52) as they should be. To be explicit, we first note that, under the phase rotation $\mathcal{H}_2 \to \mathrm{e}^{i\zeta}\mathcal{H}_2$, the electroweak Higgs basis changes as follows:

$$\begin{pmatrix}\varphi_1\\ \varphi_2\\ a\end{pmatrix} \to O_\zeta^T\begin{pmatrix}\varphi_1\\ \varphi_2\\ a\end{pmatrix} \quad \text{with} \quad O_\zeta = \begin{pmatrix}1 & 0 & 0\\ 0 & c_\zeta & s_\zeta\\ 0 & -s_\zeta & c_\zeta\end{pmatrix}, \tag{53}$$

which leads to

$$O \to O_\zeta^T O; \qquad \mathcal{M}_0^2 \to O_\zeta^T\mathcal{M}_0^2 O_\zeta \tag{54}$$

TABLE I. Classification of the conventional 2HDMs satisfying the Glashow-Weinberg condition [104] which guarantees the absence of tree-level Higgs-mediated flavor-changing neutral current (FCNC). For the four types of 2HDM, we follow the conventions found in, for example, Ref. [105].

	2HDM I	2HDM II	2HDM III	2HDM IV
ζ_u	$1/t_\beta$	$1/t_\beta$	$1/t_\beta$	$1/t_\beta$
ζ_d	$1/t_\beta$	$-t_\beta$	$1/t_\beta$	$-t_\beta$
ζ_e	$1/t_\beta$	$-t_\beta$	$-t_\beta$	$1/t_\beta$
	$\zeta_d = \zeta_e = \zeta_u$	$\zeta_d = \zeta_e = -1/\zeta_u$	$\zeta_d = -1/\zeta_e = \zeta_u$	$\zeta_d = -1/\zeta_e = -1/\zeta_u$

by observing that $(H_1, H_2, H_3)^T = O^T(\varphi_1, \varphi_2, a)^T$ and $\mathrm{diag}(M^2_{H_1}, M^2_{H_2}, M^2_{H_3}) = O^T \mathcal{M}^2_0 O$ should remain the same, respectively. Under the transformation $O \to O^T_\zeta O$, the components of the mixing matrix O change into

$$\begin{aligned} &O_{\varphi_1 i} \to O_{\varphi_1 i}, \qquad O_{\varphi_2 i} \to c_\zeta O_{\varphi_2 i} - s_\zeta O_{ai}, \\ &O_{ai} \to s_\zeta O_{\varphi_2 i} + c_\zeta O_{ai}. \end{aligned} \tag{55}$$

On the other hand, under the rotations $\zeta_f \to \mathrm{e}^{\pm i\zeta}\zeta_f$ given in Eq. (52), one may have

$$\begin{aligned} \Re\mathrm{e}(\zeta_f) &\to c_\zeta \Re\mathrm{e}(\zeta_f) \mp s_\zeta \Im\mathrm{m}(\zeta_f), \\ \Im\mathrm{m}(\zeta_f) &\to c_\zeta \Im\mathrm{m}(\zeta_f) \pm s_\zeta \Re\mathrm{e}(\zeta_f), \end{aligned} \tag{56}$$

with the upper and lower signs being for the up-type massive fermions $f = u$ and the down-type massive fermions $f = d, e$, respectively. Using Eqs. (55) and (56), it is straightforward to show that the scalar and pseudoscalar couplings given by Eq. (49) are invariant under the phase rotations of Eq. (52).

To summarize, assuming $\mathbf{y}^f_2 = \zeta_f \mathbf{y}^f_1$ with $\zeta_{f=u,d,e}$ being the three complex alignment parameters and combining Eqs. (24) and (52), we note that the Higgs potential *and* the Yukawa interactions are invariant under the following phase rotations:

$$\begin{aligned} &\mathcal{H}_2 \to \mathrm{e}^{+i\zeta}\mathcal{H}_2; \qquad Y_3 \to Y_3 \mathrm{e}^{-i\zeta}, \qquad Z_5 \to Z_5 \mathrm{e}^{-2i\zeta}, \\ &Z_6 \to Z_6 \mathrm{e}^{-i\zeta}, \qquad Z_7 \to Z_7 \mathrm{e}^{-i\zeta}; \\ &\zeta_u \to \zeta_u \mathrm{e}^{+i\zeta}, \qquad \zeta_d \to \zeta_d \mathrm{e}^{-i\zeta}, \qquad \zeta_e \to \zeta_e \mathrm{e}^{-i\zeta}, \end{aligned} \tag{57}$$

which, taking account of the CP odd tadpole condition $Y_3 + Z_6 v^2/2 = 0$, lead to *five* rephasing-invariant CPV phases in total. This leaves us more freedom to choose the input parameters for the Higgs potential other than $\mathcal{I}_{\mathrm{CPV}}$ (25), $\mathcal{I}'_{\mathrm{CPV}}$ (30), or $\mathcal{I}''_{\mathrm{CPV}}$ (31). For example, one may assign three CPV phases to the Higgs potential and take ζ_u real and positive definite. In this case, the full set of input parameter is to be

$$\begin{aligned} &\mathcal{I}^{V_\mathcal{H} \oplus \mathrm{Yukawa}}_{\mathrm{CPV}}\big|_{\zeta_u > 0, \Im\mathrm{m}(\zeta_u)=0} \\ &\quad = \{v; M_{H^\pm}, M_{H_1}, M_{H_2}, M_{H_3}, \gamma, \eta, \omega; Z_3; Z_2, Z_7\} \\ &\qquad \oplus \{|\zeta_u|, \zeta_d, \zeta_e\}, \end{aligned} \tag{58}$$

which contains 12 and 5 real degrees of freedom in the Higgs potential and the Yukawa interactions, respectively, with Z_7, ζ_d, and ζ_e being fully complex.

D. Interactions with massive vector bosons

The cubic interactions of the neutral and charged Higgs bosons with the massive gauge bosons Z and $W^\pm$ are described by the three interaction Lagrangians:

$$\begin{aligned} \mathcal{L}_{HVV} &= g M_W \left(W^+_\mu W^{-\mu} + \frac{1}{2c^2_W} Z_\mu Z^\mu \right) \sum_i g_{H_i VV} H_i, \\ \mathcal{L}_{HHZ} &= \frac{g}{2c_W} \sum_{i>j} g_{H_i H_j Z} Z^\mu (H_i \overleftrightarrow{\partial}_\mu H_j), \\ \mathcal{L}_{HH^\pm W^\mp} &= -\frac{g}{2} \sum_i g_{H_i H^+ W^-} W^{-\mu} (H_i i \overleftrightarrow{\partial}_\mu H^+) + \mathrm{H.c.}, \end{aligned} \tag{59}$$

respectively, where $X \overleftrightarrow{\partial}_\mu Y = X \partial_\mu Y - (\partial_\mu X) Y$, $i, j = 1, 2, 3$ and the normalized couplings $g_{H_i VV}$, $g_{H_i H_j Z}$, and $g_{H_i H^+ W^-}$ are given in terms of the neutral Higgs-boson 3×3 mixing matrix O by [note that $\det(O) = \pm 1$ for any orthogonal matrix O]:

$$\begin{aligned} g_{H_i VV} &= O_{\varphi_1 i}, \\ g_{H_i H_j Z} &= \mathrm{sign}[\det(O)] \epsilon_{ijk} g_{H_k VV} = \mathrm{sign}[\det(O)] \epsilon_{ijk} O_{\varphi_1 k}, \\ g_{H_i H^+ W^-} &= -O_{\varphi_2 i} + i O_{ai}, \end{aligned} \tag{60}$$

leading to the following sum rules:

$$\begin{aligned} &\sum_{i=1}^3 g^2_{H_i VV} = 1 \quad \text{and} \\ &g^2_{H_i VV} + |g_{H_i H^+ W^-}|^2 = 1 \quad \text{for each } i = 1, 2, 3. \end{aligned} \tag{61}$$

On the other hand, the quartic interactions of the neutral and charged Higgs bosons with the massive gauge bosons Z and $W^\pm$ and massless photons are given by

$$\mathcal{L}_{HHVV} = \frac{1}{v^2} \left(M^2_W W^+_\mu M^{\mu -} + \frac{M^2_Z}{2} Z_\mu Z^\mu \right) \sum_{i,j=1}^3 g_{H_i H_j VV} H_i H_j, \tag{62}$$

with $g_{H_i H_j VV} = \delta_{ij}$ and

$$\begin{aligned} \mathcal{L}_{H^+H^-VV} &= \left(\frac{g^2}{2} W^+_\mu W^{\mu -} + \frac{g^2_Z c^2_{2W}}{4} Z^\mu Z_\mu + e^2 A^\mu A_\mu \right. \\ &\qquad \left. + e g_Z c^2_{2W} A^\mu Z_\mu \right) H^+ H^-, \\ \mathcal{L}_{H^\pm HZW^\mp} &= \frac{g_Z g s^2_W}{2} \left(Z_\mu W^{-\mu} \sum_{i=1}^3 g_{ZW^-H^+H_i} H^+ H_i + \mathrm{H.c.} \right), \\ \mathcal{L}_{H^\pm HAW^\mp} &= -\frac{eg}{2} \left(A_\mu W^{-\mu} \sum_{i=1}^3 g_{AW^-H^+H_i} H^+ H_i + \mathrm{H.c.} \right), \end{aligned} \tag{63}$$

with $g_{ZW^-H^+H_i} = g_{AW^-H^+H_i} = -O_{\varphi_2 i} - i O_{ai}$, $c_{2W} = \cos 2\theta_W$, and $g_Z = g/c_W = e/(s_W c_W)$.

III. CONSTRAINTS

In this Section, we consider the perturbative unitarity (UNIT) conditions and those for the Higgs potential to be bounded from below (BFB) to obtain the primary theoretical constraints on the potential parameters or, equivalently, the constraints on the Higgs-boson masses including correlations among them and the mixing among the three neutral Higgs bosons. We further consider the constraints on the Higgs masses and their couplings with vector bosons taking into account the electroweak oblique corrections to the so-called S and T parameters. We emphasize that all the three types of constraints from the perturbative unitarity, the Higgs potential bounded from below, and the electroweak precision observables (EWPOs) are independent of the basis chosen and working in the Higgs basis does not invoke any restrictions. We also consider the constraints on $|\zeta_e|$, $|\zeta_u|$, and the product of $\zeta_u\zeta_d$ taking account of the charged Higgs contributions to the flavor-changing τ decays into light leptons, $Z \to b\overline{b}$, ϵ_K, and $b \to s\gamma$ [96,106].[12]

A. Perturbative unitarity

For the unitarity conditions, we closely follow Ref. [108] [13] considering the three scattering matrices of $\mathcal{M}^S_{1,2,3}$ which are expressed in terms of the quartic couplings Z_{1-7}, see also Ref. [109]. The two 4×4 real and symmetric scattering matrices $\mathcal{M}^S_1$ and $\mathcal{M}^S_2$ are given by

$$\mathcal{M}^S_1 = \begin{pmatrix} \eta_{00} - I & \eta^T \\ \eta & E + I\times \mathbf{1}_{3\times3} \end{pmatrix};$$
$$\mathcal{M}^S_2 = \begin{pmatrix} 3\eta_{00} - I & 3\eta^T \\ 3\eta & 3E + I\times \mathbf{1}_{3\times3} \end{pmatrix}, \tag{64}$$

where $\eta_{00} = Z_1 + Z_2 + Z_3$ and $I = Z_3 - Z_4$. The row vector η^T is given by

$$\eta^T = (\Re\mathrm{e}(Z_6 + Z_7), -\Im\mathrm{m}(Z_6 + Z_7), Z_1 - Z_2), \tag{65}$$

and the 3×3 real and symmetric matrix E by

$$E = \begin{pmatrix} Z_4 + 2\Re\mathrm{e}(Z_5) & -2\Im\mathrm{m}(Z_5) & \Re\mathrm{e}(Z_6 - Z_7) \\ -2\Im\mathrm{m}(Z_5) & Z_4 - 2\Re\mathrm{e}(Z_5) & -\Im\mathrm{m}(Z_6 - Z_7) \\ \Re\mathrm{e}(Z_6 - Z_7) & -\Im\mathrm{m}(Z_6 - Z_7) & Z_1 + Z_2 - Z_3 \end{pmatrix}. \tag{66}$$

The third 3×3 scattering matrix $\mathcal{M}^S_3$ is Hermitian which takes the form of

$$\mathcal{M}^S_3 = \begin{pmatrix} 2Z_1 & 2Z_5 & \sqrt{2}Z_6 \\ 2Z^*_5 & 2Z_2 & \sqrt{2}Z^*_7 \\ \sqrt{2}Z^*_6 & \sqrt{2}Z_7 & Z_3 + Z_4 \end{pmatrix}. \tag{67}$$

Then, the unitarity conditions are imposed by requiring that the 11 eigenvalues of the three scattering matrices $\mathcal{M}^S_{1,2,3}$ and the quantity I should have their moduli smaller than 4π.

When $Z_6 = Z_7 = 0$, the 12 unitarity conditions simplify into

$$\begin{aligned} |Z_3 \pm Z_4| &< 4\pi, \\ |Z_3 \pm 2|Z_5|| &< 4\pi, \\ |Z_3 + 2Z_4 \pm 6|Z_5|| &< 4\pi, \\ |Z_1 + Z_2 \pm \sqrt{(Z_1 - Z_2)^2 + 4|Z_5|^2}| &< 4\pi, \\ |Z_1 + Z_2 \pm \sqrt{(Z_1 - Z_2)^2 + Z_4^2}| &< 4\pi, \\ |3Z_1 + 3Z_2 \pm \sqrt{9(Z_1 - Z_2)^2 + (2Z_3 + Z_4)^2}| &< 4\pi. \end{aligned} \tag{68}$$

While taking $Z_1 = Z_2 = Z_3 = Z_4 = Z_5 = 0$, one may have

$$\begin{aligned} \sqrt{|Z_6|^2 + |Z_7|^2} &< 2\sqrt{2}\pi, \\ \sqrt{|Z_6|^2 + |Z_7|^2 + |Z_6^2 + Z_7^2|} &< \frac{4\pi}{3}. \end{aligned} \tag{69}$$

Then, by combining them, one may arrive at the following UNIT conditions for individual parameters [108]:

$$\begin{aligned} &|Z_{1,2,5}| < 2\pi/3, \quad |Z_{6,7}| < 2\sqrt{2}\pi/3, \\ &|Z_3 - Z_4| < 4\pi \cup |2Z_3 + Z_4| < 4\pi \cup |Z_3 + 2Z_4| < 4\pi. \end{aligned} \tag{70}$$

B. Higgs potential bounded-from-below

We consider the following 5 necessary conditions for the most general 2HDM Higgs potential with explicit CP violation to be bounded-from-below in a marginal sense [108][14]:

$$\begin{aligned} Z_1 \geq 0, \quad Z_2 \geq 0; \\ 2\sqrt{Z_1 Z_2} + Z_3 \geq 0, \quad 2\sqrt{Z_1 Z_2} + Z_3 + Z_4 - 2|Z_5| \geq 0; \\ Z_1 + Z_2 + Z_3 + Z_4 + 2|Z_5| - 2|Z_6 + Z_7| \geq 0. \end{aligned} \tag{71}$$

Note that though the quartic couplings Z_2 and Z_7 have no direct relations to the masses and mixing of Higgs bosons

[12] We refer to, for example, Ref. [107] for an extensive study of flavor observables in the conventional 2HDMs taking the Φ basis.

[13] We keep our conventions for the potential parameters.

[14] Denoting the quartic part of the scalar potential as V_4, a marginal stability requirement means that $V_4 \geq 0$ for any direction in field space tending to infinity [75]. In contrast, a strong stability requirement is $V_4 > 0$ without the equality sign. In this work, we adopt the marginal stability requirement.

but they are interrelated with the other five quartic couplings of $Z_{1,3-6}$ through the UNIT and BFB conditions.

C. Electroweak precision observables

The electroweak oblique corrections to the so-called S, T, and U parameters [110,111] provide significant constraints on the quartic couplings of the 2HDM. Fixing $U=0$ which is suppressed by an additional factor $M_Z^2/M_{\rm BSM}^2$[15] compared to S and T, the S and T parameters are constrained as follows:

$$\frac{(S-\hat{S}_0)^2}{\sigma_S^2}+\frac{(T-\hat{T}_0)^2}{\sigma_T^2}-2\rho_{ST}\frac{(S-\hat{S}_0)(T-\hat{T}_0)}{\sigma_S\sigma_T} \leq R^2(1-\rho_{ST}^2), \tag{72}$$

with $R^2=2.3, 4, 61, 5.99, 9.21, 11.83$ at 68.3%, 90%, 95%, 99%, and 99.7% confidence levels (CLs), respectively. For our numerical analysis, we adopt the 95% CL limits. The central values and their standard deviations are given by[16]

$$(\hat{S}_0,\sigma_S)=(0.00,0.07), \qquad (\hat{T}_0,\sigma_T)=(0.05,0.06), \tag{73}$$

with a strong correlation $\rho_{ST}=0.92$ between S and T parameters. The electroweak oblique parameters, which are defined to arise from new physics only, are in excellent agreement with the SM values of zero for the reference values of $M_{H_{\rm SM}}=125.25$ GeV and $M_t=172.5$ GeV [112].

In 2HDM, the S and T parameters might be estimated using the following expressions [113,114]:

$$S_\Phi=-\frac{1}{4\pi}\left[(1+\delta_{\gamma Z}^{H^\pm})^2F'_\Delta(M_{H^\pm},M_{H^\pm}) -\sum_{(i,j)=(1,2)}^{(1,3),(2,3)}(g_{H_iH_jZ}+\delta_Z^{H_iH_j})^2F'_\Delta(M_{H_i},M_{H_j})\right],$$

$$T_\Phi=-\frac{\sqrt{2}G_F}{16\pi^2\alpha_{\rm EM}}\left[-\sum_{i=1}^{3}|g_{H_iH^-W^+}+\delta_W^{H_i}|^2F_\Delta(M_i,M_{H^\pm}) +\sum_{(i,j)=(1,2)}^{(1,3),(2,3)}(g_{H_iH_jZ}+\delta_Z^{H_iH_j})^2F_\Delta(M_{H_i},M_{H_j})\right]. \tag{74}$$

In this work, we ignore the vertex corrections $\delta_{\gamma Z}^{H^\pm}$, $\delta_Z^{H_iH_j}$, and $\delta_W^{H_i}$ since the size of the most of the quartic couplings are smaller than 3 and the quantum corrections proportional to $\sim Z_i^2/16\pi^2$ might be negligible. Then, we observe that all the relevant couplings are determined by the three physical couplings of g_{H_iVV} since $g_{H_iH_jZ}^2=|\epsilon_{ijk}|g_{H_kVV}^2=|\epsilon_{ijk}|O_{\varphi_1 k}^2$ and $|g_{H_iH^-W^+}|^2=1-g_{H_iVV}^2=1-O_{\varphi_1 i}^2$. The one-loop functions are given by[17]

$$F_\Delta(m_0,m_1)=F_\Delta(m_1,m_0)=\frac{m_0^2+m_1^2}{2}-\frac{m_0^2m_1^2}{m_0^2-m_1^2}\ln\frac{m_0^2}{m_1^2},$$

$$F'_\Delta(m_0,m_1)=F'_\Delta(m_1,m_0) =-\frac{1}{3}\left[\frac{4}{3}-\frac{m_0^2\ln m_0^2-m_1^2\ln m_1^2}{m_0^2-m_1^2} -\frac{m_0^2+m_1^2}{(m_0^2-m_1^2)^2}F_\Delta(m_0,m_1)\right]. \tag{75}$$

We note that $F_\Delta(m,m)=0$ and $F'_\Delta(m,m)=\frac{1}{3}\ln m^2$.[18] When $g_{H_1VV}^2=1$, neglecting the Z^2-dependent vertex correction factors $\delta_{\gamma Z}^{H^\pm}$, $\delta_W^{H_i}$, and $\delta_Z^{H_iH_j}$, S_Φ and T_Φ are symmetric under the exchange $M_{H_2}\leftrightarrow M_{H_3}$ and they are identically vanishing when $M_{H_2}=M_{H_3}=M_{H^\pm}$.[19]

D. Flavor constraints on the alignment parameters

The alignment parameters $\zeta_{f=u,d,e}$ are constrained by considering the charged Higgs contributions to the low energy observables such as flavor-changing τ decays, leptonic and semileptonic decays of pseudoscalar mesons, the $Z\to b\bar{b}$ process, B meson mixing, the CPV parameter ϵ_K in K meson mixing, and the radiative $b\to s\gamma$ decay [96]. In this work, we consider the flavor constraints on the absolute sizes of ζ_e, ζ_u, and ζ_d. Note that, we neglect the constraints on the products of the alignment parameters taking account of only the single constraints on the absolute values of ζ_e, ζ_u, and ζ_d under the assumption that they are fully independent from each other.

The flavor-changing τ decays into light leptons provide the following constraint on $|\zeta_e|$ [96]:

$$|\zeta_e|\leq 200\left(\frac{M_{H^\pm}}{500\ \text{GeV}}\right), \tag{76}$$

at 95% CL. On the other hand, the constraint on $|\zeta_u|$ may come from the Z-peak precision observables involving the $Z\to b\bar{b}$ decay assuming the quantum corrections to the $Zb\bar{b}$ vertex beyond the SM is dominated by the charged Higgs contributions. More explicitly, the ratio $R_b=\Gamma(Z\to b\bar{b})/\Gamma(Z\to\text{hadrons})$ is used by neglecting the contributions depending on $|\zeta_d|$ which are suppressed by the factor $\bar{m}_t(M_Z)/\bar{m}_b(M_Z)\sim 60$ compared to those depending on

[15]Here, $M_{\rm BSM}$ denotes some heavy mass scale involved with new physics beyond the Standard Model.

[16]See the 2020 edition of the review "*10. Electroweak Model and Constraints on New Physics*" by J. Erler and A. Freitas in Ref. [112].

[17]See, for example, Ref. [115].

[18]Here and after, $\ln m^2$ could be understood as, for example, $\ln[m^2/(1\ \text{GeV})^2]$ if necessary.

[19]The S_Φ and T_Φ parameters are independent of M_{H_1} when $g_{H_1VV}^2=1$.

$|\zeta_u|$. It turns out that the upper limit on $|\zeta_u|$ linearly increases with $M_{H^\pm}$ as follows [96]:

$$|\zeta_u| \leq 0.72 + 1.19\left(\frac{M_{H^\pm}}{500\ \text{GeV}}\right) \quad (95\%\ \text{CL}). \quad (77)$$

To be very strict, the above upper limit should be applied only when $|\zeta_d| = 0$. The similar while more direct upper limit $|\zeta_u|$ could be obtained by considering the CPV parameter ϵ_K in K meson mixing which depends on $|\zeta_u|$ only neglecting the masses of the light d and s quarks. Actually the limit from ϵ_K is slightly stronger than that from $Z \to b\bar{b}$ by the amount of about 10% [96]. In this work, for the upper limit on $|\zeta_u|$, we apply the slightly weaker constraint from $Z \to b\bar{b}$ given by Eq. (77) while considering it valid independently of ζ_d. In passing, for the $\Delta B = 2$ processes mediated by box diagrams with exchanges of $W^\pm$ and/or $H^\pm$ bosons, we note that the leading Wilson coefficients which are not suppressed by the light quark mass depend ζ_u and ζ_d. When $\zeta_d = 0$, one might obtain the similar upper limit on $|\zeta_u|$ as that from ϵ_K [96].

There is no limit on ζ_d independently of ζ_u and/or ζ_e, but one may extract some interesting information on ζ_d considering the radiative $b \to s\gamma$ decay. Numerically, the decay amplitude can be cast into the following form [106,116][20]:

$$\mathcal{A} \sim \mathcal{A}_{\text{SM}}\left\{1 - 0.1\zeta_u\zeta_d\left(\frac{500\ \text{GeV}}{M_{H^\pm}}\right)^2 + 0.01|\zeta_u|^2\left(\frac{500\ \text{GeV}}{M_{H^\pm}}\right)^2\right\}. \quad (78)$$

When $\zeta_u\zeta_d$ is negative, the interference with the SM amplitude is always constructive and the product is constrained to be small and, as usual, $|\zeta_d|$ can be significantly larger (smaller) than 1 only when $|\zeta_u|$ is very small (large). On the contrary, if $\zeta_u\zeta_d$ is positive, $|\zeta_d|$ could be large independently of $|\zeta_u|$. In this case, a destructive interference occurs and the experimental constraints can be satisfied when

$$\zeta_u\zeta_d \sim 20\left(\frac{M_{H^\pm}}{500\ \text{GeV}}\right)^2. \quad (79)$$

Combining the upper limit on $|\zeta_u|$ given by Eq. (77), we observe that the destructive interference can always occur when

$$|\zeta_d| \gtrsim 20\frac{\left(\frac{M_{H^\pm}}{500\ \text{GeV}}\right)^2}{0.72 + 1.19\left(\frac{M_{H^\pm}}{500\ \text{GeV}}\right)}, \quad (80)$$

and $\zeta_u\zeta_d > 0$. Most generally, allowing $\zeta_u\zeta_d$ to be complex, it turns out that the rough 95% CL upper limit on the absolute value of the product is basically saturated by the relation given by Eq. (79) [96] or

$$|\zeta_u||\zeta_d| \lesssim 20\left(\frac{M_{H^\pm}}{500\ \text{GeV}}\right)^2 \quad (95\%\ \text{CL}). \quad (81)$$

For the summary, we present the upper limits on $|\zeta_e|$, $|\zeta_u|$, and $|\zeta_e\zeta_d|$ and the lower limit on $|\zeta_d|$ in Fig. 1.

Before closing this section, we briefly comment on the constraints from the heavy Higgs boson searches carried out at the LHC. The heavy neutral Higgs bosons have been searched through their decays into $\tau^+\tau^-$ [117–120], $b\bar{b}$ [121], $t\bar{t}$ [122–124], WW [125], ZZ [126–129], $Zh_{125\ \text{GeV}}$ [130,131], etc. On the other hand, the charged Higgs boson search channels include the decay modes into $\tau^\pm\nu$ [132,133], tb [134–136], cb [137], cs [138,139], and $Wh_{125\ \text{GeV}}$ [130]. Basically, the experimental upper limits on the product of the production cross section and the decay rate into a specific search mode have been analyzed to obtain the allowed parameter space of a specific model. For example, the search in the $\tau^+\tau^-$ final state excludes the presence of a heavy neutral Higgs with M_A below about 1 TeV at 95% CL in the minimal supersymmetric extension of the SM (MSSM) when, depending on scenarios, $\tan\beta \gtrsim 15 \sim 25$ and the exclusion contour reaches up to $M_A = 1.6$ TeV for $\tan\beta = 60$ [118]. While in the aligned 2HDM taken in this work, the Yukawa couplings of the up- and down-type quarks and the charged leptons to heavy Higgs bosons are completely uncorrelated and the interpretation of the experimental limits is much more involved. This is because the three alignment parameters of $\zeta_{u,d,e}$ are independent from each other while all of them are involved in the calculation of the decay rate pertinent to a specific search mode. In principle, one can easily avoid the constraints from, for example, $H/A \to \tau\tau$ and $H^\pm \to \tau\nu$ by taking $|\zeta_e| \ll 1$, but it might be still allowed to have $|\zeta_e| \gtrsim 20$ and $M_A < 1$ TeV if one can suppress the branching fraction into $\tau^+\tau^-$ by choosing the other alignment parameters of ζ_u and ζ_d appropriately. In this respect, a thorough analysis of the experimental search results in the framework of aligned 2HDM with three independent alignment parameters deserves an independent full consideration. In this work, we simply assume that the parameter space considered in the next Section could be made more or less safe from the LHC constraints from no observation of significant excess in the heavy Higgs boson searches by judiciously manipulating the three alignment parameters which are otherwise uncorrelated.

[20]Note that the product $\zeta_u\zeta_d$ is the rephasing invariant quantity in our convention, see Eq. (52).

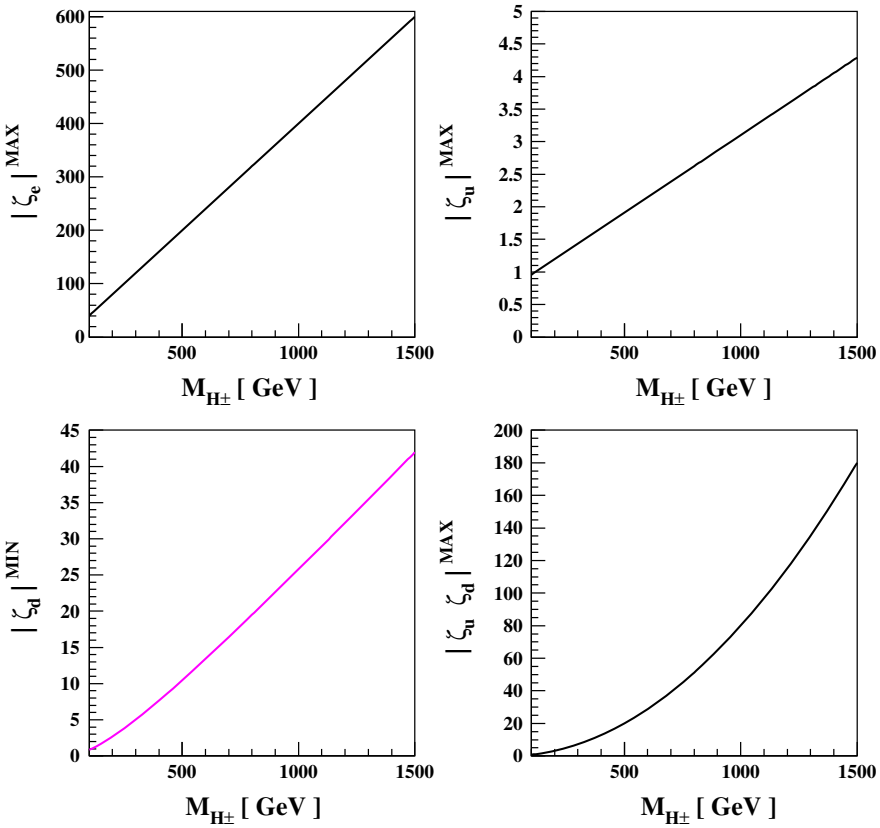

FIG. 1. The 95% CL limits on the alignment parameters as functions of $M_{H^\pm}$ obtained by considering the charged Higgs contributions to low energy observables [96]. (Upper Left) The upper limit on $|\zeta_e|$ from flavor-changing τ decays into light leptons, see Eq. (76). (Upper Right) The upper limit on $|\zeta_u|$ from R_b and ϵ_K, see Eq. (77). (Lower Left) The minimum value of $|\zeta_d|$ required to satisfy the $b \to s\gamma$ constraint through the destructive interference when $\zeta_u\zeta_d$ is positive, see Eq. (80). The R_b and ϵ_K constraints on $|\zeta_u|$ are combined. (Lower Right) The upper limit on the product of $|\zeta_u|$ and $|\zeta_d|$ from $b \to s\gamma$ when ζ_u and ζ_d are complex, see Eq. (81).

IV. NUMERICAL ANALYSIS

From the relation $g_{H_1VV} = O_{\varphi_1 1}$ given in Eq. (60) and the expressions for the H_i couplings to the two SM fermions given in Eq. (49), one might define the Yukawa delay factor $\Delta_{H_1\bar{f}f}$ by the amount of which the decoupling of the Yukawa couplings of the lightest Higgs boson is delayed compared to its coupling to a pair of massive vector bosons:

$$\begin{aligned}\Delta_{H_1\bar{f}f} &\equiv \sqrt{(g^S_{H_1\bar{f}f} - g_{H_1VV})^2 + (g^P_{H_1\bar{f}f})^2} \\ &= |\zeta_f|(1 - g^2_{H_1VV})^{1/2},\end{aligned} \tag{82}$$

where we use the relation $\sum_{\alpha=\varphi_1,\varphi_2,a} O^2_{\alpha i} = 1$ for $i = 1$. We observe that the delay factor $\Delta_{H_1\bar{f}f}$ defined above is basis-independent and can be generally used even in the CPV case. Anticipating that the impacts on the Yukawa delay factor due to the CP-violating phases of $Z_{5,6,7}$ and $\zeta_{u,d,e}$ are redundant, we consider the CP-conserving (CPC) case for our numerical study for simplicity. For a recent global analysis of the aligned CPC 2HDM taking account of several phenomenological constraints as well as theoretical requirements, we refer to Ref. [140] but with a caution.[21]

A. UNIT and BFB constraints

First of all, we consider the UNIT and BFB constraints. Observing that the two conditions depend only on the quartic couplings Z_{1-7}, we take the following set of input parameters[22]:

$$\mathcal{I}^Z_{\rm CPC} = \{v, Y_2; Z_1, Z_2, Z_3, Z_4, Z_5, Z_6, Z_7\}. \tag{83}$$

[21]In Ref. [140], the authors take $\lambda_{5,6,7}$ for the fitting parameters in addition to the Higgs masses $m_h = 125.10$ GeV, M_H, M_A, $M_{H^\pm}$, and the mixing angle $\tilde{\alpha}$. In our notations, they use the set of input parameters of $\{v; M_{H^\pm}, M_h, M_H, M_A, \gamma; Z_5, Z_6, Z_7\}$. Comparing to $\mathcal{I}'_{\rm CPC}$ given in Eq. (23), we find that the potential parameters Z_5 and Z_6 are used more than needed while Z_2 and Z_3 are missing in the set. Note that Z_5 and Z_6 are entirely fixed when the mixing angle and the three neutral Higgs masses are given, see Eq. (22), and the parameter Z_2 should be included at least because it is independent of the Higgs masses and mixing like as Z_7.

[22]To have $\mathcal{I}^Z_{\rm CPC}$ from Eq. (18), we trade $M_{H^\pm}$ with Z_3. Note that the dimensionful parameter Y_2 is irrelevant for the UNIT and BFB constraints.

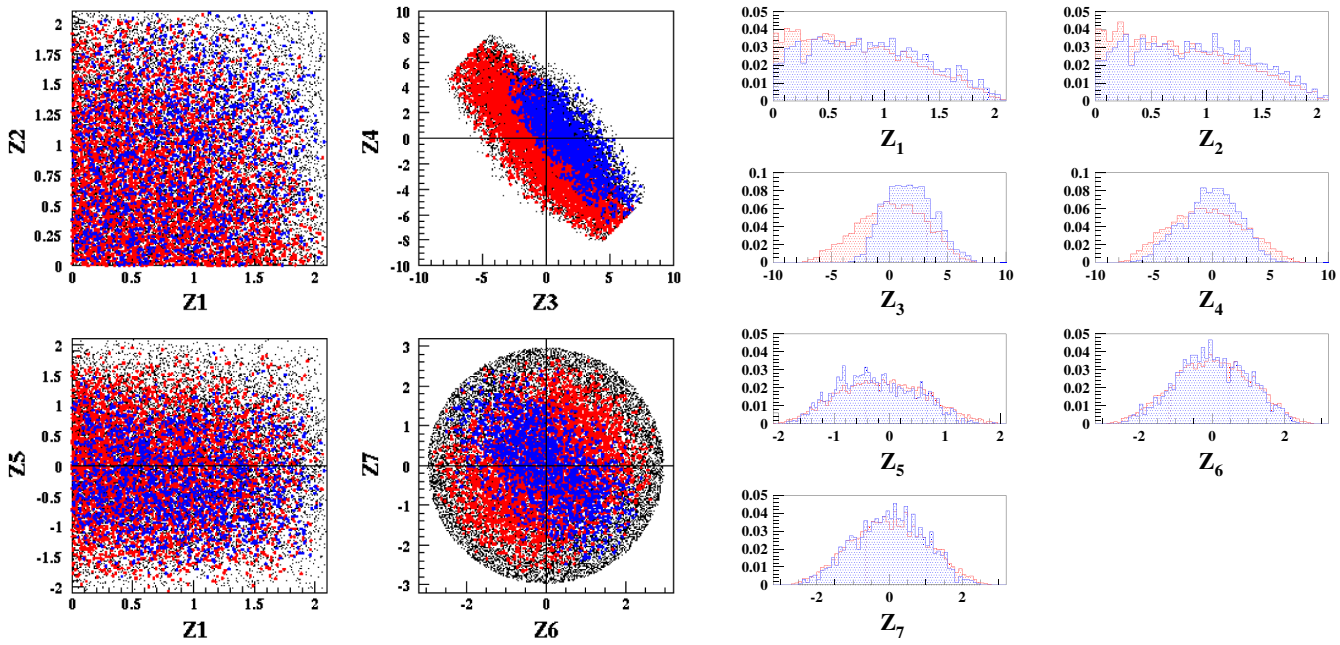

FIG. 2. The *UNIT* and *BFB* constraints using $\mathcal{I}^Z_{\rm CPC}$, see Eq. (83): (Left) Scatter plots (red) of Z_2 versus Z_1 (upper left), Z_4 versus Z_3 (upper right), Z_5 versus Z_1 (lower left), and Z_7 versus Z_6 (lower right) with the UNIT conditions imposed. For the blue points, the necessary BFB conditions are additionally imposed. Also shown are the points in black which are obtained by requiring only the simplified UNIT conditions in Eqs. (68) and (69). (Right) The normalized distributions of the quartic couplings obtained by requiring only the UNIT (red) and the combined UNIT ⊕ BFB conditions.

In the left panel of Fig. 2, we show the scatter plots of Z_2 versus Z_1 (upper left), Z_4 versus Z_3 (upper right), Z_5 versus Z_1 (lower left), and Z_7 versus Z_6 (lower right). The plots are produced by randomly generating the quartic couplings in the $\mathcal{I}^Z_{\rm CPC}$ set. In each plot, the black points are obtained by imposing only the simplified UNIT conditions of Eqs. (68) and (69). The full consideration of the UNIT conditions based on the scattering matrices $\mathcal{M}^S_{1,2,3}$ produces the red points. The results obtained by simultaneously imposing the full UNIT and BFB conditions (UNIT ⊕ BFB) are denoted by the blue points. We find our results are very consistent with those presented in Ref. [108]. After imposing the UNIT and UNIT ⊕ BFB conditions, we note that the normalized distributions of the quartic couplings are no longer flat as shown in the right panel of Fig. 2. As in the left panel, the distributions of the quartic couplings obtained by requiring only the UNIT (red) conditions and the combined UNIT ⊕ BFB conditions are in red and blue, respectively. We note that the smaller $|Z_6 + Z_7|$ and the positive Z_3 values are preferred by further imposing the BFB conditions in addition to the UNIT ones, see Eq. (71).

B. Electroweak constraints

Coming to the electroweak (ELW) constraints, since the oblique corrections are expressed in terms of the masses and couplings of Higgs bosons, it is more natural and convenient to take the following set of input parameters:

$$\mathcal{I}'_{\rm CPC} = \{v; M_{H^\pm}, M_h = M_{H_1}, M_H, M_A, \gamma; Z_3; Z_2, Z_7\}, \quad (84)$$

referring to Eq. (23). In the $\mathcal{I}'_{\rm CPC}$ set, all the massive parameters are physical Higgs masses except $v = (\sqrt{2}G_F)^{-1/2} \simeq 246.22$ GeV. We assume that the neutral state $h = H_1$ is the lightest Higgs boson and plays the role of the SM Higgs boson in the decoupling limit of $s_\gamma = 0$ by taking $M_{H_1} = 125.5$ GeV [76], and, for the masses of heavy Higgs bosons, we randomly generate their masses squared between $M^2_{H_1}$ and $(1.5\ \text{TeV})^2$. For the mixing angle γ, we take the convention of $|\gamma| \le \pi/2$ without loss of generality resulting in $c_\gamma \ge 0$ and $\text{sign}(s_\gamma) = \text{sign}(Z_6)$. For the implementation of the UNIT and BFB constraints using the set $\mathcal{I}'_{\rm CPC}$, we recall the quartic couplings $Z_{1,4,5,6}$ in terms of the Higgs masses and the mixing angle γ in the CPC case given by Eq. (22).

Using the set $\mathcal{I}'_{\rm CPC}$ for the input parameters in the CPC case, the S and T parameters given by Eq. (74) take the following simpler forms:

$$\begin{aligned} S^{\rm CPC}_\Phi &= -\frac{1}{4\pi}[F'_\Delta(M_{H^\pm}, M_{H^\pm}) - c^2_\gamma F'_\Delta(M_A, M_H) \\ &\quad - s^2_\gamma F'_\Delta(M_A, M_h)], \\ T^{\rm CPC}_\Phi &= \frac{\sqrt{2}G_F}{16\pi^2\alpha_{\rm EM}}[F_\Delta(M_A, M_{H^\pm}) + c^2_\gamma F_\Delta(M_H, M_{H^\pm}) \\ &\quad + s^2_\gamma F_\Delta(M_h, M_{H^\pm}) - c^2_\gamma F_\Delta(M_A, M_H) \\ &\quad - s^2_\gamma F_\Delta(M_A, M_h)], \end{aligned} \quad (85)$$

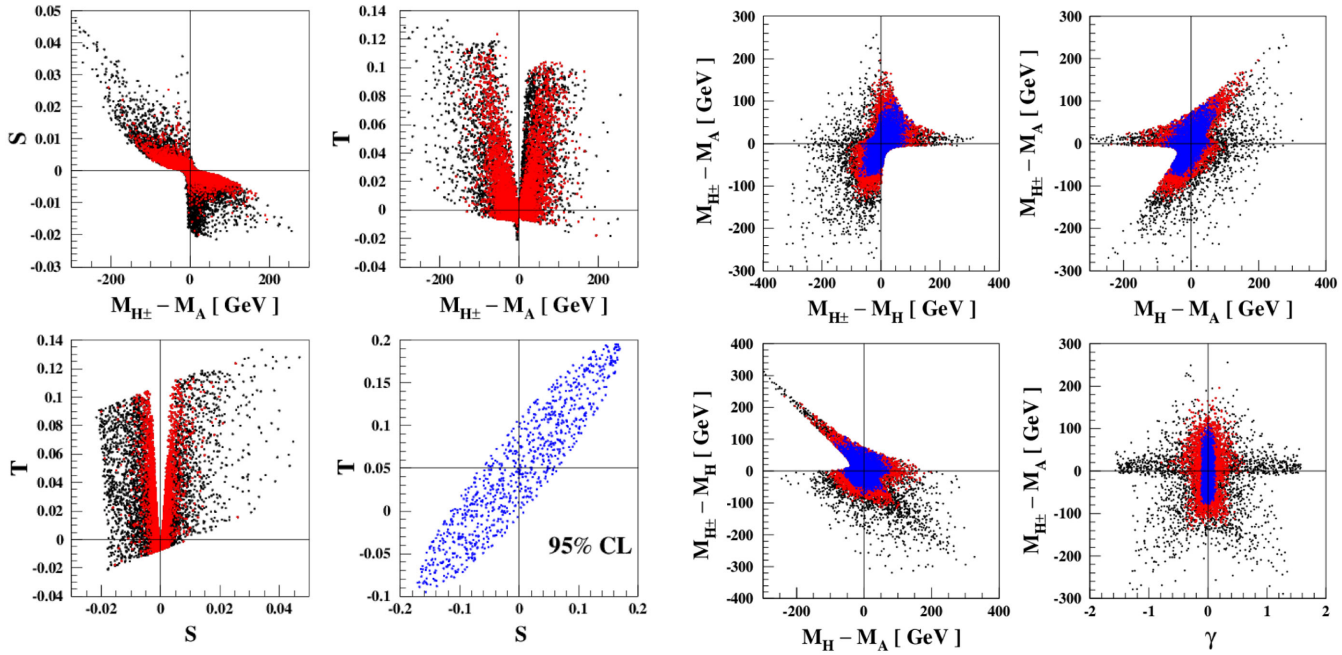

FIG. 3. Correlations among the S and T parameters, mass differences, and the mixing angle γ using the set $\mathcal{I}'_{\rm CPC}$. (Left) Scatter plots of S versus $M_{H^\pm} - M_A$ (upper left), T versus $M_{H^\pm} - M_A$ (upper right), and T versus S (lower left) with the combined UNIT $\oplus$ BFB $\oplus$ ELW$_{95\%}$ constraints imposed (black). The red points are with the small angle condition $|\gamma| < 0.1$. In the lower-right plot, as a reference, the 95% CL ELW constraint on the S and T parameters according to Eqs. (72) and (73) is shown. (Right) Scatter plots of $M_{H^\pm} - M_A$ versus $M_{H^\pm} - M_H$ (upper left), $M_{H^\pm} - M_A$ versus $M_H - M_A$ (upper right), $M_{H^\pm} - M_H$ versus $M_H - M_A$ (lower left), and $M_{H^\pm} - M_A$ versus γ (lower right) with the combined UNIT $\oplus$ BFB $\oplus$ ELW$_{95\%}$ constraints imposed (black). The red and blue points are for $M_{H^\pm} > 500$ GeV and $M_{H^\pm} > 1$ TeV, respectively.

ignoring the vertex corrections. We observe that $T_\Phi^{\rm CPC}$ is identically vanishing when $M_{H^\pm} = M_A$ and, when $M_{H^\pm} \sim M_A \sim M_H \gg M_h$, we obtain[23]

$$S_\Phi^{\rm CPC} \simeq -\frac{1}{4\pi}\left[\frac{\ln M_{H^\pm}^2}{3} - c_\gamma^2\left(\frac{\ln M_A^2}{3} + \frac{M_H - M_A}{3M_A}\right) - s_\gamma^2\left(\frac{\ln M_A^2}{3} - \frac{5}{18}\right)\right],$$
$$T_\Phi^{\rm CPC} \simeq \frac{\sqrt{2}G_F}{16\pi^2\alpha_{\rm EM}}\left[\frac{2(M_A - M_{H^\pm})^2}{3} + c_\gamma^2\frac{2(M_H - M_{H^\pm})^2}{3} + s_\gamma^2\frac{M_{H^\pm}^2}{2} - c_\gamma^2\frac{2(M_A - M_H)^2}{3} - s_\gamma^2\frac{M_A^2}{2}\right], \quad (86)$$

keeping the leading terms. To obtain Eq. (86) for the approximated expressions of the S and T parameters, we use

$$F_\Delta(m_0, m_1) = \frac{2(m_0 - m_1)^2}{3} - \frac{(m_0 - m_1)^4}{30m_1^2} + \mathcal{O}\left[\frac{(m_0 - m_1)^5}{m_1^3}\right],$$
$$F'_\Delta(m_0, m_1) = \frac{\ln m_1^2}{3} + \frac{(m_0 - m_1)}{3m_1} - \frac{(m_0 - m_1)^2}{30m_1^2} + \mathcal{O}\left[\frac{(m_0 - m_1)^3}{m_1^3}\right], \quad (87)$$

for $m_0 \sim m_1$ and

$$F_\Delta(m_0, m_1) = \frac{m_1^2}{2} + \left(\frac{1}{2} + \ln\frac{m_0^2}{m_1^2}\right)m_0^2 + \mathcal{O}\left[\left(\frac{m_0^4}{m_1^2}\right)\ln\frac{m_0^2}{m_1^2}\right],$$
$$F'_\Delta(m_0, m_1) = \frac{\ln m_1^2}{3} - \frac{5}{18} + \frac{2}{3}\frac{m_0^2}{m_1^2} + \mathcal{O}\left[\left(\frac{m_0^4}{m_1^4}\right)\ln\frac{m_0^2}{m_1^2}\right], \quad (88)$$

for $m_1 \gg m_0$.

In the left panel of Fig. 3, we show the S and T parameters imposing the UNIT, BFB, and ELW constraints abbreviated by the combined UNIT $\oplus$ BFB $\oplus$ ELW$_{95\%}$ ones. Note that the 95% CL ELW limits are adopted and the heavy Higgs masses squared are scanned up to $(1.5\ \text{TeV})^2$. We find that S takes values in the range between -0.02 and 0.05 whose absolute values are smaller than $\sigma_S = 0.07$, see Eq. (73).

[23]For S_Φ, note that $[\ln M_A^2/3 + (M_H - M_A)/3M_A] - [\ln M_H^2/3 + (M_A - M_H)/3M_H] \simeq (M_H - M_A)^3/9M_A^3$.

Actually, we find that $|S| < \sigma_S$ even with only the UNIT and BFB constraints imposed. Note that S is mostly negative (positive) when $M_{H^\pm} > (<) M_A$. Specifically, we find that $S \simeq -1/4\pi(5/18) \simeq -0.02$ when $M_{H^\pm} - M_A = 0$ and $\gamma = \pi/2$. The T parameter takes its value between -0.02 and 0.13 which are given by the delimited range determined by $-0.02 < S < 0.05$, the strong correlation $\rho_{ST} = 0.92$ and $R^2_{95\%} = 5.99$, see Eqs. (72) and (73) and the lower-right plot in the left panel of Fig. 3. Incidentally, we observe that $T = 0$ when $M_{H^\pm} = M_A$ though it quickly deviates from 0 when $M_{H^\pm} \neq M_A$. In the right panel of Fig. 3, we show the correlations among the mass differences and the mixing angle γ using the set $\mathcal{I}'_{\rm CPC}$. We find that

$$\begin{aligned} |M_H - M_A|/\text{GeV} &\lesssim 200(100), \\ |M_{H^\pm} - M_H|/\text{GeV} &\lesssim 200(110), \\ |M_{H^\pm} - M_A|/\text{GeV} &\lesssim 200(110), \\ |\gamma| &\lesssim 0.8(0.14), \end{aligned} \tag{89}$$

when $M_{H^\pm} \gtrsim 500$ GeV (1 TeV).

We show the correlations among the heavy Higgs-boson masses and the mixing angle γ in the left panel of Fig. 4. Requiring the ELW constraint in addition to the UNIT $\oplus$ BFB ones, we find that Z_1 and γ take values near to 0 and Z_4 and Z_5 positive ones more likely, see the right panel of Fig. 4. We find that the UNIT and BFB conditions combined with the ELW constraint restrict the quartic couplings as follows:

$$\begin{aligned} 0.1 \lesssim Z_1 \lesssim 2.0, \quad & 0 \lesssim Z_2 \lesssim 2.1, \\ -2.4 \lesssim Z_3 \lesssim 8.0, \quad & -6.3 \lesssim Z_4 \lesssim 6.0, \\ -1.9 \lesssim Z_5 \lesssim 1.6, \quad & -2.7 \lesssim Z_6 \lesssim 2.7, \\ -2.7 \lesssim Z_7 \lesssim 2.7. & \end{aligned} \tag{90}$$

C. Alignment of Yukawa couplings

Now, we have come to the point to address the alignment of Yukawa couplings. When we talk about the alignment of the Yukawa couplings in general 2HDMs, we imply: (*i*) the alignment of them in the flavor space and (*ii*) the alignment of the lightest Higgs-boson couplings to a pair of the SM fermions in the decoupling limit of $M_{H,A,H^\pm} \to \infty$. By (*i*), we precisely mean the assumption that the two Yukawa matrices of $\mathbf{y}^f_1$ and $\mathbf{y}^f_2$ are aligned in the flavor space or $\mathbf{y}^f_2 = \zeta_f \mathbf{y}^f_1$, see Eq. (45), which, in the CPC case, leads to

$$g^S_{H_1 \bar{f} f} = O_{\varphi_1 1} + \zeta_f O_{\varphi_2 1} = c_\gamma - \zeta_f s_\gamma, \tag{91}$$

with $f = u$ and d for the up- and down-type quarks, respectively, and $f = e$ for the three charged leptons. Then, by (*ii*), one might mean

$$g^S_{H_1 \bar{f} f} \to 1 \quad \text{as } M_{H,A,H^\pm} \to \infty. \tag{92}$$

In Eq. (91), we note that the quantity c_γ is nothing but the coupling $g_{H_1 VV} = O_{\varphi_1 1} = c_\gamma$ which is driven to take the

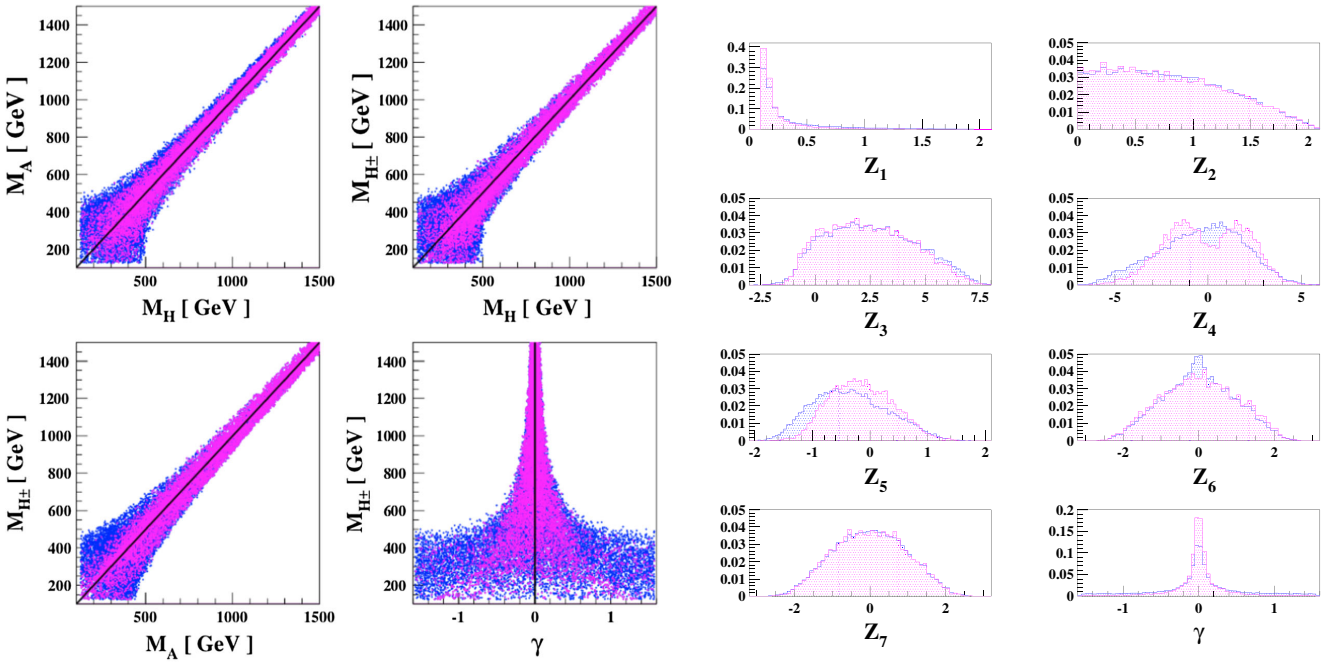

FIG. 4. The UNIT $\oplus$ BFB $\oplus$ ELW$_{95\%}$ constraints (magenta) using $\mathcal{I}'_{\rm CPC}$, see Eq. (84). For comparisons, we also show the results after applying only the UNIT $\oplus$ BFB constraints (blue).: (Left) Scatter plots of M_A versus M_H (upper left), $M_{H^\pm}$ versus M_H (upper right), $M_{H^\pm}$ versus M_A (lower left), and $M_{H^\pm}$ versus γ (lower right). (Right) The normalized distributions of the quartic couplings and the mixing angle γ.

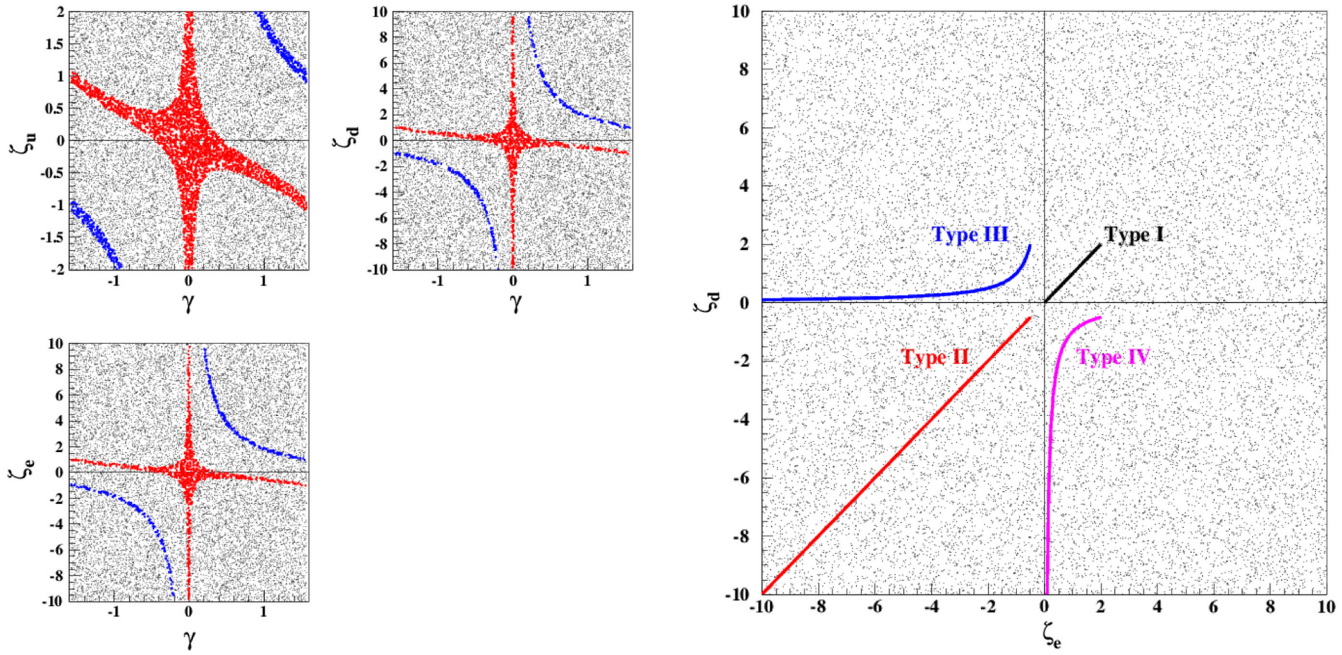

FIG. 5. (Left) Scatter plots of ζ_u versus γ (upper left), ζ_d versus γ (upper right), and ζ_e versus γ (lower left) obtained by scanning $-\pi/2 \le \gamma \le \pi/2$ and the three real parameters of the set $\mathcal{I}^{\zeta}_{\rm CPC}$ in the ranges of $-2 < \zeta_u < 2$ and $-10 < \zeta_{d,e} < 10$. On each $\zeta_f - \gamma$ plane, the regions satisfying $|g^S_{H_1\bar{f}f} - 1| < 0.1$ and $|g^S_{H_1\bar{f}f} + 1| < 0.1$ are denoted in red and blue, respectively. (Right) Scatter plot of ζ_d versus ζ_e with $1/100 < \zeta_u < 2$. The four lines represent the four conventional 2HDMs as denoted taking $1/2 < t_\beta < 100$.

SM value of 1 by the combined UNIT, BFB, and ELW constraints as $M_{H,A,H^\pm}$ increases. Therefore, from Eq. (82), the Yukawa delay factor simplifies to $\Delta_{H_1\bar{f}f} = |\zeta_f s_\gamma|$, and the alignment of the lightest Higgs-boson couplings to the SM fermions in the decoupling limit is delayed by the amount of $|\zeta_f s_\gamma|$ which can not be ignored even when $|s_\gamma| \ll 1$ if $|\zeta_f|$ is significantly larger than 1.

For a quantitative study, in addition to $\mathcal{I}'_{\rm CPC}$ given by Eq. (84), we have added the following set of input parameters containing three real parameters:

$$\mathcal{I}^{\zeta}_{\rm CPC} = \{\zeta_u, \zeta_d, \zeta_e\}. \tag{93}$$

In the left panel of Fig. 5, we show the correlations between each of the three alignment parameters $\zeta_{f=u,d,e}$ and the mixing angle γ when the absolute value of the corresponding coupling $g^S_{H_1\bar{f}f}$ is within 10% range of the SM value of 1 or $|g^S_{H_1\bar{f}f} - 1| < 0.1$ and $|g^S_{H_1\bar{f}f} + 1| < 0.1$ for $g^S_{H_1\bar{f}f} > 0$ (red) and $g^S_{H_1\bar{f}f} < 0$ (blue), respectively. Scanning $|\gamma| \le \pi/2$, $g^S_{H_1\bar{f}f} \simeq 1$ near $\gamma = 0$. At $\gamma = \pm\pi/2$, the $g^S_{H_1\bar{f}f}$ coupling takes the value of 1 when $\zeta_f = \mp 1$ (red). While if $\zeta_f = \pm 1$, we note that $g^S_{H_1\bar{f}f} = -1$ at $\gamma = \pm\pi/2$ (blue). In the right panel of Fig. 5, by the four lines, we show the correlations between ζ_d and ζ_e in the four conventional 2HDMs[24] based on appropriately defined discrete Z_2 symmetries taking $1/100 < \zeta_u = 1/t_\beta < 2$, see Table I. We observe that both ζ_d and ζ_e are bounded *only* in the type-I 2HDM between $1/100$ and 2. Otherwise, at least one of them is limitless in principle. Therefore, except the type-I 2HDM, $g^S_{H_1\bar{d}d}$ and/or $g^S_{H_1\bar{e}e}$ could be largely deviated from 1 in the decoupling limit even when ζ_u is limited.

To concentrate on the alignment of the lightest Higgs-boson couplings to a pair of the SM fermions in the decoupling limit of $M_{H,A,H^\pm} \to \infty$ under the assumption of $\mathbf{y}^f_2 \propto \mathbf{y}^f_1$ as in Eq. (45), we consider a simplified scenario in which the mixing angle $|\sin\gamma|$ is inversely proportional to $1/M^2_{H^\pm}$ reflecting the behavior of $|\sin\gamma| = |g_{HVV}|$ being suppressed by the quartic powers of the heavy Higgs-boson masses at leading order [141]. In the upper-left frame of Fig. 6, we show the scatter plot for $|\gamma|$ versus $M_{H^\pm}$ together with the three curves showing the cases of $\sin\gamma = (125\,\text{GeV}/M_{H^\pm})^2$ (black), $\sin\gamma = (200\,\text{GeV}/M_{H^\pm})^2$ (red), and $\sin\gamma = (350\ \text{GeV}/M_{H^\pm})^2$ (blue) from bottom to top.[25] The input parameters are the same as in Fig. 4

[24]The parameters ζ_d and ζ_e are completely uncorrelated in the general 2HDM based on the relation Eq. (45) as shown by the scattered black dots in the right panel of Fig. 5.

[25]The choice of $\sin\gamma = (m_6/M_{H^\pm})^2$ is equivalent to fix $Z_6 = (M^2_H - m^2_h)\cos\gamma\sin\gamma/v^2 \sim (m_6/v)^2$ when $M_H \sim M_{H^\pm} \gg M_h$ and $\sin(\gamma) \ll 1$, see Eq. (22).

and the combined UNIT ⊕ BFB ⊕ $\mathrm{ELW}_{95\%}$ constraints are imposed. For illustration, we take the case of $\sin\gamma = (200\ \mathrm{GeV}/M_{H^\pm})^2$. The coupling of the lightest Higgs boson H_1 to a pair of massive vector bosons are constrained by the precision LHC Higgs data [46]. We note that, for example, $\cos\gamma = g_{H_1VV} \gtrsim 0.95$ or $|\sin\gamma| = |g_{HVV}| \lesssim 0.3$ can be satisfied when $M_{H^\pm} \gtrsim 400$ GeV for this choice. We further assume that the masses of the heavy Higgs bosons of H, A, and $H^\pm$ are degenerate. This assumption reflects the fact that the combined UNIT ⊕ BFB ⊕ $\mathrm{ELW}_{95\%}$ constraints prefers quite degenerate heavy-Higgs bosons when they weigh more than about 400 GeV as shown in the left panel of Fig. 4. We dub this scenario **SCN200** in which we precisely fix and vary the input parameters in the two sets of $\mathcal{I}'_{\mathrm{CPC}}$ and $\mathcal{I}^{\zeta}_{\mathrm{CPC}}$ as follows:

$$\begin{aligned}\textbf{SCN200}:\ &\{M_h = M_{H_1} = 125.5\ \mathrm{GeV}, M_H = M_A = M_{H^\pm} = [200\ldots1500]\ \mathrm{GeV};\\ &\sin\gamma = \pm(200\ \mathrm{GeV}/M_{H^\pm})^2; Z_2 = [0\ldots2], Z_3 = [-3\ldots8], Z_7 = [-3\ldots3]\}\\ &\oplus \{\zeta_u = [1/100\ldots2], \zeta_d = [-100\ldots100], \zeta_e = [-100\ldots100]\},\end{aligned} \tag{94}$$

together with the combined UNIT ⊕ BFB ⊕ $\mathrm{ELW}_{95\%}$ constraints imposed. In this scenario, the Yukawa delay factor is given by

$$\Delta_{H_1\bar{f}f}|_{\mathbf{SCN200}} = |\zeta_f|\frac{(200\ \mathrm{GeV})^2}{M^2_{H^\pm}} \simeq |\zeta_f|\frac{|Z_6|v^2}{M^2_{H^\pm}}, \tag{95}$$

with $Z_6|_{\mathbf{SCN200}} \simeq 0.66$. Note that, we use the approximation $Z_6 v^2 = (M_H^2 - M_h^2)c_\gamma s_\gamma \simeq M^2_{H^\pm} s_\gamma$ in the above equation.

In the upper-right frame of Fig. 6, we show the scatter plot of $g^S_{H_1\bar{u}u}$ versus $M_{H^\pm}$ taking **SCN200** in which the upper limit on $|\zeta_u|$ from R_b and ϵ_K is applied, see Eq. (77). We observe that the coupling $g^S_{H_1\bar{u}u}$ is within about 30% and 10% ranges of the SM value of 1 when $M_{H^\pm} > 500$ GeV and $M_{H^\pm} > 1$ TeV, respectively. As previously discussed, the alignment of the coupling $g^S_{H_1\bar{f}f}$ is delayed by the amount of $\zeta_f \sin\gamma$ compared to the coupling g_{H_1VV} and $g^S_{H_1\bar{u}u}$ is most deviated from its SM value of 1 by the amount of

$$\begin{aligned}\Delta_{H_1\bar{u}u}|_{\mathbf{SCN200},|\zeta_u|\le2} &= |\zeta_u|\left(\frac{200\ \mathrm{GeV}}{M_{H^\pm}}\right)^2\\ &\le 0.32\left(\frac{500\ \mathrm{GeV}}{M_{H^\pm}}\right)^2.\end{aligned} \tag{96}$$

To make this point clear, we add the blue and red lines showing $g^S_{H_1\bar{u}u}$ taking $\zeta_u = 0.2$, 1, and 2 and the magenta one showing g_{H_1VV}. We indeed see that $g^S_{H_1\bar{u}u}$ is most close to g_{H_1VV} when $\zeta_u = 0.2$ and the two lines taking $\zeta_u = 2$ provide the envelope which includes all the scattered points.[26] In the lower frames of Fig. 6, the scatter plots of $g^S_{H_1\bar{d}d}$ versus $M_{H^\pm}$ (left) and $g^S_{H_1\bar{e}e}$ versus $M_{H^\pm}$ (right) are shown. They are basically the same since ζ_d and ζ_e are varied in the same range of $[-100, 100]$. And the same arguments are applied as in the case of $g^S_{H_1\bar{u}u}$: the lines with $\zeta_{d,e} = 0.5$ are most close to g_{H_1VV} among the blue and red lines and those with $\zeta_{d,e} = 100$ provide the envelopes which include all the scattered points. We see that $g^S_{H_1\bar{d}d}$ and $g^S_{H_1\bar{e}e}$ can be largely deviated from their SM values of 1 when $|\zeta_{d,e}|$ is large:

$$\begin{aligned}&\Delta_{H_1\bar{d}d,H_1\bar{e}e}|_{\mathbf{SCN200},|\zeta_d|\le100,|\zeta_e|\le100}\\ &\quad= |\zeta_{d,e}|\left(\frac{200\ \mathrm{GeV}}{M_{H^\pm}}\right)^2 \lesssim 1.8\left(\frac{1.500\ \mathrm{TeV}}{M_{H^\pm}}\right)^2.\end{aligned} \tag{97}$$

Incidentally, we observe that the constraint on $|\zeta_e|$ from the flavor-changing τ decays into light leptons excludes the region with $|g^S_{H_1\bar{e}e}| \gtrsim 60$ and $M_{H^\pm} \lesssim 250$ GeV which is not seen in the window chosen for the scatter plot of $g^S_{H_1\bar{e}e}$ versus $M_{H^\pm}$ in Fig. 6, see Eq. (76).

Of course, the alignment parameters $\zeta_{d,e}$ are constrained by the precision LHC Higgs data. From the observation that the absolute values of the couplings of the SM-like H_1 to a pair of bottom quarks and tau leptons are required to be consistent with 1 within about 10% at 1σ level [46], one might have $|g^S_{H_1\bar{d}d} \pm 1| \lesssim 0.1$ and $|g^S_{H_1\bar{e}e} \pm 1| \lesssim 0.1$.[27] For the positive sign, the condition $|g^S_{H_1\bar{d}d} - 1| < 0.1$ constrains $|\zeta_d| \lesssim 6$, see the red points in the left panel of Fig. 7. On the other hand $g^S_{H_1\bar{d}d} \sim -1$ allows the larger values of ζ_d given by $\zeta_d = (1+\cos\gamma)/\sin\gamma \simeq \pm 2M^2_{H^\pm}/(200\ \mathrm{GeV})^2$, see the

[26] Note that the line segments for $\zeta_u = 2$ with $M_{H^\pm} \lesssim 500$ GeV are located outside the scattered region implying that they are excluded by the upper limit on $|\zeta_u|$ from R_b and ϵ_K.

[27] The negative value of $g^S_{H_1\bar{d}d} \sim -1$ is less preferred than the positive one $g^S_{H_1\bar{d}d} \sim +1$ at the level of about 1.5σ considering the b-quark loop contributions to the H_1 coupling to two gluons [46]. While, for $g^S_{H_1\bar{e}e}$, the current data precision is yet insufficient to tell its sign. In this work, we consider both signs for $g^S_{H_1\bar{d}d}$ and $g^S_{H_1\bar{e}e}$.

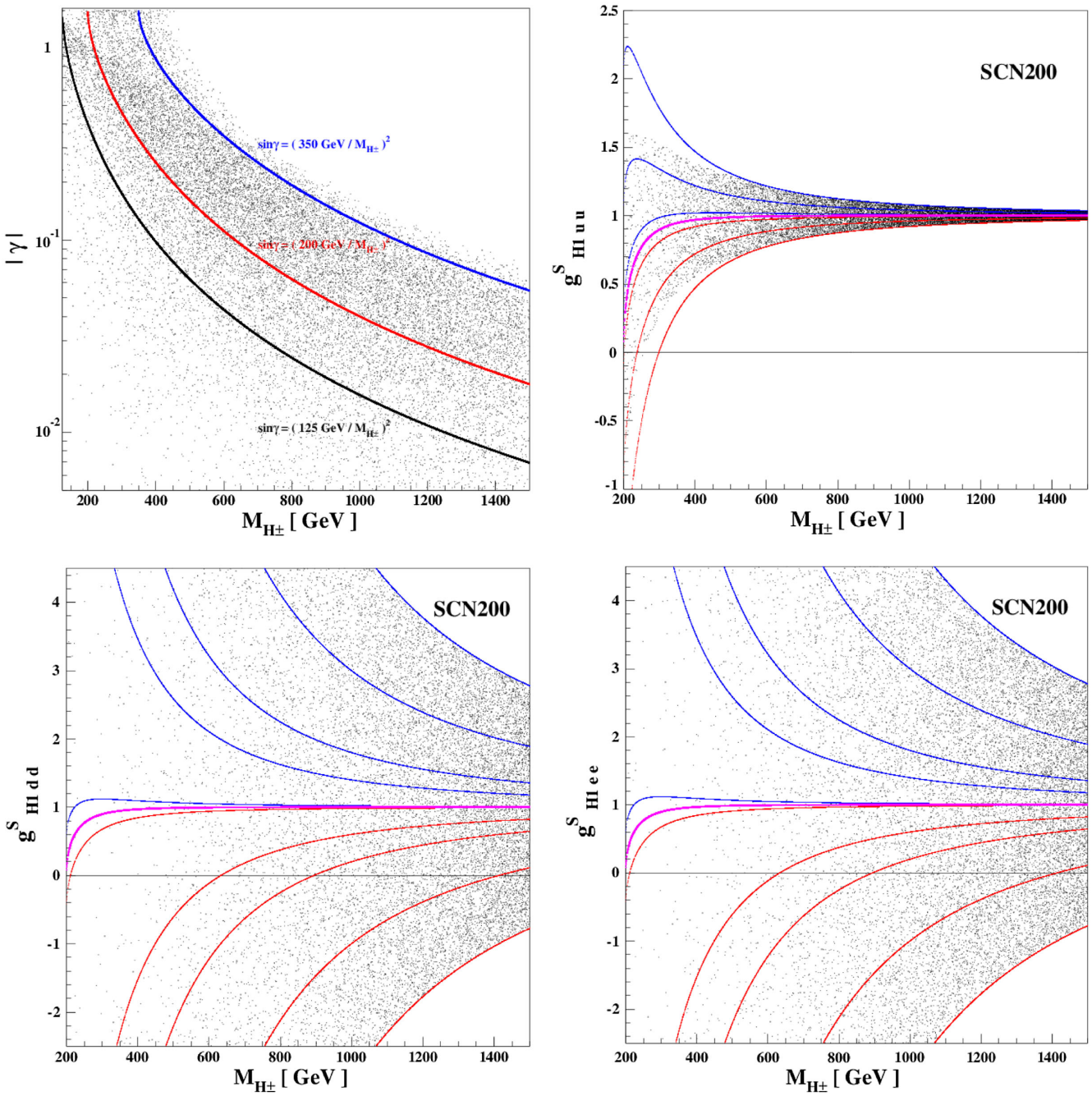

FIG. 6. (Upper Left) The same as in the lower-right plot in the left panel of Fig. 4 but for $|\gamma|$ versus $M_{H^\pm}$ with the UNIT $\oplus$ BFB $\oplus$ ELW$_{95\%}$ constraints imposed. The three curves show the cases of $|\sin\gamma| = (125\ \text{GeV}/M_{H^\pm})^2$ (black), $|\sin\gamma| = (200\ \text{GeV}/M_{H^\pm})^2$ (red), and $|\sin\gamma| = (350\ \text{GeV}/M_{H^\pm})^2$ (blue) from bottom to top. (Upper Right) Scatter plot of $g^S_{H_1\bar{u}u}$ versus $M_{H^\pm}$ taking **SCN200** in which the upper limit on $|\zeta_u|$ from R_b and ϵ_K is applied, see Eq. (77). The blue (red) lines are for $\cos\gamma + (-)\zeta_u|\sin\gamma|$ for $\zeta_u = 2, 1, 0.2$ from the outermost lines to the magenta one which is for $g_{H_1VV} = \cos\gamma$. (Lower Left) Scatter plot of $g^S_{H_1\bar{d}d}$ versus $M_{H^\pm}$ taking **SCN200**. The blue (red) lines are for $\cos\gamma + (-)\zeta_d|\sin\gamma|$ for $\zeta_d = 100, 50, 20, 10, 0.5$ from the outermost lines to the magenta one which is for $g_{H_1VV} = \cos\gamma$. (Lower Right) The same as in the lower-left plot but for $g^S_{H_1\bar{e}e}$ versus $M_{H^\pm}$ with the lines for $\cos\gamma \pm \zeta_e|\sin\gamma|$ for $\zeta_e = 100, 50, 20, 10, 0.5$.

blue points in the left panel of Fig. 7. In the same panel for ζ_d versus $M_{H^\pm}$, we also show the lower limit on $|\zeta_d|$ from $b \to s\gamma$ through the destructive interference by the magenta lines, see Eq. (80) and the lower-left panel of Fig. 1. We observe that the two regions with $|g^S_{H_1\bar{d}d} + 1| < 0.1$ are mostly outside the band delimited by the two magenta lines implying that large values of $|\zeta_d|$ for $g^S_{H_1\bar{d}d} \sim -1$ are hardly constrained by $b \to s\gamma$. For $g^S_{H_1\bar{e}e}$, the same arguments are

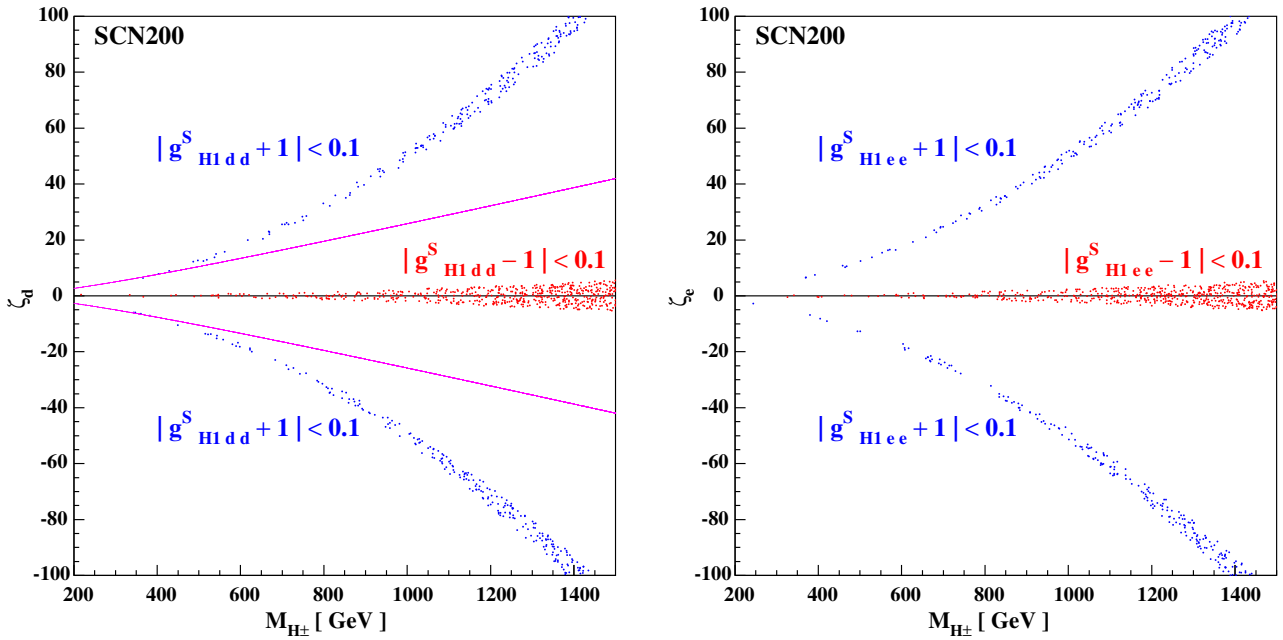

FIG. 7. Scatter plots of ζ_d versus $M_{H^\pm}$ (left) and ζ_e versus $M_{H^\pm}$ (right) taking **SCN200**. The red and blue points denote the regions where $g^S_{H_1\bar{d}d}$ and $g^S_{H_1\bar{e}e}$ are within the 10% ranges of the values of 1 and -1, respectively. The magenta lines in the left panel denote $|\zeta_d|^{\rm MIN}$ required to satisfy the $b \to s\gamma$ constraint through the destructive interference when $\zeta_u\zeta_d$ is positive, see Eq. (80) and the lower-left panel of Fig. 1.

applied, see the right panel of Fig. 7. Note that the constraints from the flavor-changing τ decays into light leptons given by Eq. (76) are too weak to affect those on $g^S_{H_1\bar{e}e}$ by the precision LHC Higgs data.

Lastly, we comment on the wrong-sign alignment limit in the four types of conventional 2HDMs in which the H_1 couplings to the down-type quarks and/or those to the charged leptons are equal in strength but opposite in sign to the corresponding SM ones. The two couplings $g^S_{H_1\bar{d}d}$ and $g^S_{H_1\bar{e}e}$ are completely independent from each other in general 2HDM, but, in the conventional four types of 2HDMs, they are related. We observe that the couplings are given by either $\cos\gamma - \sin\gamma/t_\beta$ or $\cos\gamma + t_\beta \sin\gamma$ in any type of 2HDMs, see Table I. In this case, $\cos\gamma - \sin\gamma/t_\beta = \pm 1$ for the t_β value which makes $\cos\gamma + t_\beta \sin\gamma = \mp 1$. This implies that, independently of 2HDM type and regardless of the heavy Higgs-mass scale, all four types of 2HDMs could be viable against the LHC Higgs precision data in the *wrong-sign* alignment limit.

V. CONCLUSIONS

We have studied the alignment of Yukawa couplings in the framework of general 2HDMs identifying the lightest neutral Higgs boson as the 125 GeV one discovered at the LHC. We take the so-called Higgs basis [73,74,88–92] for the Higgs potential in which only one of the two doublets contains the nonvanishing vacuum expectation value v. For the Yukawa couplings, rather than invoking the Glashow-Weinberg condition [104] based on appropriately defined discrete Z_2 symmetries, we require the absence of tree-level FCNCs by assuming that the Yukawa matrices describing the couplings of the two Higgs doublets to the SM fermions are aligned in the flavor space [93–95].

For a numerical study, we further assume that the seven quartic couplings $Z_{i=1-7}$ appearing in the Higgs potential and the three alignment parameters $\zeta_{f=u,d,e}$ for Yukawa couplings are all real by anticipating that the impacts due to CP-violating phases of $Z_{5,6,7}$ and ζ_f's on the alignment of Yukawa couplings are redundant. In this case, in addition to the vev v and masses of the SM fermions, the model can be fully described by specifying the following set of 11 free parameters:

$$\{M_h = M_{H_1} = 125.5\,\text{GeV}, M_H, M_A, M_{H^\pm}, \gamma, Z_2, Z_3, Z_7; \zeta_u, \zeta_d, \zeta_e\},$$

where $M_{h,H}$ (with $M_h < M_H$) and M_A denote the masses of CP-even and CP-odd neutral Higgs bosons, respectively, and the mixing between the two CP-even neutral states is described by the angle γ. The quartic couplings $Z_{1,4,5,6}$ are determined in terms of $M_{h,H,A}$, $M_{H^\pm}$, γ, and v. The quartic coupling Z_3 is related to the massive parameter Y_2 appearing in the Higgs potential through $Y_2 = M^2_{H^\pm} - Z_3 v^2/2$. On the other hand, the other quartic couplings Z_2 and Z_7 have no direct relevance to the masses and mixing of Higgs bosons, but we observe that they are interrelated with the other five

quartic couplings of $Z_{1,3-6}$ through the perturbative unitarity (UNIT) conditions and those for the Higgs potential to be bounded from below (BFB). We note that the UNIT and BFB conditions are basis-independent, i.e., the same in any basis [108]. Also considered are the constraints from the electroweak (ELW) oblique corrections to the S and T parameters which are expressed in terms of the physical observable quantities of $M_{h,H,A}$, $M_{H^\pm}$, and g_{H_iVV} which are again invariant under a change of basis [84]. We further consider the constraints on the alignment parameters $\zeta_{f=u,d,e}$ from flavor-changing τ decays, R_b, ϵ_K, and the radiative $b \to s\gamma$ decay.

For the independent model parameters and the rephasing invariant combinations of CP-violating phases, among the several points already discussed in the literature, we highlight the following ones:

(1) The general 2HDM potential can be fully specified with the masses of the charged and three neutral Higgs bosons, the orthogonal neutral-Higgs boson mixing matrix $O_{3\times3}$ and the three dimensionless quartic couplings of $Z_{2,3,7}$ in addition to the vev v.

(2) For the CP phases, as far as the Higgs potential *and* the three complex alignment parameters for the Yukawa couplings are involved, the Lagrangians are invariant under the following phase rotations:

$$\begin{aligned}&\mathcal{H}_2 \to e^{+i\zeta}\mathcal{H}_2;\\ &Y_3 \to Y_3 e^{-i\zeta}, \quad Z_5 \to Z_5 e^{-2i\zeta},\\ &Z_6 \to Z_6 e^{-i\zeta}, \quad Z_7 \to Z_7 e^{-i\zeta};\\ &\zeta_u \to \zeta_u e^{+i\zeta}, \quad \zeta_d \to \zeta_d e^{-i\zeta}, \quad \zeta_e \to \zeta_e e^{-i\zeta},\end{aligned} \tag{98}$$

which, taking account of the CP odd tadpole condition $Y_3 + Z_6 v^2/2 = 0$, lead to the following five rephasing-invariant CPV phases:

$$\begin{aligned}&\mathrm{Arg}[Z_6(Z_5^*)^{1/2}], \quad \mathrm{Arg}[Z_7(Z_5^*)^{1/2}]; \quad \mathrm{Arg}[\zeta_u(Z_5)^{1/2}],\\ &\mathrm{Arg}[\zeta_d(Z_5^*)^{1/2}], \text{ and } \mathrm{Arg}[\zeta_e(Z_5^*)^{1/2}],\end{aligned} \tag{99}$$

pivoting, for example, around the complex quartic coupling Z_5.

Incidentally, it is well known that the 3 alignment parameters are the same $\zeta_u = \zeta_d = \zeta_e = 1/t_\beta$ in the type-I 2HDM. In this case, they cannot be significantly larger than 1 since $t_\beta \ll 1$ leads to a nonperturbative top-quark Yukawa coupling and a Landau pole close to the TeV scale. Therefore, in the type-I model among the 4 conventional 2HDMs, all the Yukawa couplings of the lightest Higgs boson most quickly approach the corresponding SM values as the masses of the heavy neutral Higgs bosons increase and their decouplings are least delayed.

We further suggest the following points as the main results specifically pertinent to our analysis:

(1) By scanning the heavy Higgs masses up to 1.5 TeV, we find that the UNIT and BFB conditions combined with the ELW constraint restrict the quartic couplings as follows:

$$\begin{aligned}&0.1 \lesssim Z_1 \lesssim 2.0, \qquad 0 \lesssim Z_2 \lesssim 2.1,\\ &-2.4 \lesssim Z_3 \lesssim 8.0, \qquad -6.3 \lesssim Z_4 \lesssim 6.0,\\ &-1.9 \lesssim Z_5 \lesssim 1.6, \qquad -2.7 \lesssim Z_6 \lesssim 2.7,\\ &-2.7 \lesssim Z_7 \lesssim 2.7,\end{aligned} \tag{100}$$

and, when $M_{H^\pm} \gtrsim 500$ GeV (1 TeV), we also find that

$$\begin{aligned}|M_H - M_A|/\mathrm{GeV} &\lesssim 200(100),\\ |M_{H^\pm} - M_H|/\mathrm{GeV} &\lesssim 200(110),\\ |M_{H^\pm} - M_A|/\mathrm{GeV} &\lesssim 200(110),\\ |\gamma| &\lesssim 0.8(0.14).\end{aligned} \tag{101}$$

(2) As the masses of heavy Higgs bosons increase, compared to the g_{H_1VV} coupling of the lightest Higgs boson to a pair of massive vector bosons, the decoupling of the Yukawa couplings to the lightest Higgs boson is delayed by the amount of the Yukawa delay factor $\Delta_{H_1\bar{f}f} = |\zeta_f|(1 - g^2_{H_1VV})^{1/2}$ which is basis-independent and can be generally used even in the presence of CPV phases. Therefore, though g_{H_1VV} approaches its SM value of 1 very quickly as the masses of heavy Higgs bosons increase, the coupling of H_1 to a pair of fermions can significantly deviate from its SM value if $|\zeta_f|$ is large. Note that $|\zeta_u|$ is constrained to be small by R_b and ϵ_K, see Eq. (77). While $|\zeta_d|$ and $|\zeta_e|$ are constrained to be small by the LHC precision Higgs data when the corresponding Yukawa couplings are with the similar strength and the same sign as the SM ones, but it could be large when the Yukawa coupling takes the wrong sign.

(3) The wrong-sign alignment, in which the H_1 couplings to a pair of f-type fermions are equal in strength but opposite in sign to the corresponding SM ones, occurs when $\zeta_f = (1 + \cos\gamma)/\sin\gamma$ independently of the heavy Higgs-boson masses. In the conventional four types of 2HDMs, $\zeta_f = -t_\beta$ or $1/t_\beta$ and the Yukawa couplings are given by either $\cos\gamma - \sin\gamma/t_\beta$ or $\cos\gamma + t_\beta \sin\gamma$ in any type of 2HDMs. We observe that $\cos\gamma - \sin\gamma/t_\beta = \mp 1$ for the t_β value making $\cos\gamma + t_\beta \sin\gamma = \pm 1$ and any type of conventional 2HDMs is viable against the LHC Higgs precision data.

(4) Last but not least, by combining with the upper limit on $|\zeta_u|$ from R_b and ϵ_K, we derive the *lower* limit on $|\zeta_d|$ independently of ζ_u and ζ_e when the non-SM

contribution to $b \to s\gamma$ is about two times of the SM one at the amplitude level.

ACKNOWLEDGMENTS

We thank Seong Youl Choi for helpful comments on the manuscript. This work was supported by the National Research Foundation (NRF) of Korea Grant No. NRF-2021R1A2B5B02087078 (J. S. L., J. P.). In addition, the work of J. S. L. was supported in part by the NRF of Korea Grant No. NRF-2022R1A5A1030700 and the work of J. P. was supported in part by the NRF of Korea Grant No. NRF-2018R1D1A1B07051126.

[1] G. Aad *et al.* (ATLAS Collaboration), Observation of a new particle in the search for the Standard Model Higgs boson with the ATLAS detector at the LHC, Phys. Lett. B **716**, 1 (2012).
[2] S. Chatrchyan *et al.* (CMS Collaboration), Observation of a new boson at a mass of 125 GeV with the CMS experiment at the LHC, Phys. Lett. B **716**, 30 (2012).
[3] D. Carmi, A. Falkowski, E. Kuflik, and T. Volansky, Interpreting LHC Higgs results from natural new physics perspective, J. High Energy Phys. 07 (2012) 136.
[4] A. Azatov, R. Contino, and J. Galloway, Model-independent bounds on a light Higgs, J. High Energy Phys. 04 (2012) 127; 04 (2013) 140(E).
[5] J. R. Espinosa, C. Grojean, M. Muhlleitner, and M. Trott, Fingerprinting Higgs suspects at the LHC, J. High Energy Phys. 05 (2012) 097.
[6] M. Klute, R. Lafaye, T. Plehn, M. Rauch, and D. Zerwas, Measuring Higgs Couplings from LHC Data, Phys. Rev. Lett. **109**, 101801 (2012).
[7] D. Carmi, A. Falkowski, E. Kuflik, and T. Volansky, Interpreting the 125 GeV Higgs, Nuovo Cimento C **035**, 315 (2012).
[8] I. Low, J. Lykken, and G. Shaughnessy, Have we observed the Higgs (imposter)?, Phys. Rev. D **86**, 093012 (2012).
[9] P. P. Giardino, K. Kannike, M. Raidal, and A. Strumia, Is the resonance at 125 GeV the Higgs boson?, Phys. Lett. B **718**, 469 (2012).
[10] J. Ellis and T. You, Global analysis of the Higgs candidate with mass ~125 GeV, J. High Energy Phys. 09 (2012) 123.
[11] J. R. Espinosa, C. Grojean, M. Muhlleitner, and M. Trott, First glimpses at Higgs' face, J. High Energy Phys. 12 (2012) 045.
[12] D. Carmi, A. Falkowski, E. Kuflik, T. Volansky, and J. Zupan, Higgs after the discovery: A status report, J. High Energy Phys. 10 (2012) 196.
[13] S. Banerjee, S. Mukhopadhyay, and B. Mukhopadhyaya, New Higgs interactions and recent data from the LHC and the Tevatron, J. High Energy Phys. 10 (2012) 062.
[14] F. Bonnet, T. Ota, M. Rauch, and W. Winter, Interpretation of precision tests in the Higgs sector in terms of physics beyond the Standard Model, Phys. Rev. D **86**, 093014 (2012).
[15] T. Plehn and M. Rauch, Higgs couplings after the discovery, Europhys. Lett. **100**, 11002 (2012).
[16] A. Djouadi, Precision Higgs coupling measurements at the LHC through ratios of production cross sections, Eur. Phys. J. C **73**, 2498 (2013).
[17] B. A. Dobrescu and J. D. Lykken, Coupling spans of the Higgs-like boson, J. High Energy Phys. 02 (2013) 073.
[18] G. Cacciapaglia, A. Deandrea, G. Drieu La Rochelle, and J. B. Flament, Higgs couplings beyond the standard model, J. High Energy Phys. 03 (2013) 029.
[19] G. Belanger, B. Dumont, U. Ellwanger, J. F. Gunion, and S. Kraml, Higgs couplings at the end of 2012, J. High Energy Phys. 02 (2013) 053.
[20] G. Moreau, Constraining extra-fermion(s) from the Higgs boson data, Phys. Rev. D **87**, 015027 (2013).
[21] T. Corbett, O. J. P. Eboli, J. Gonzalez-Fraile, and M. C. Gonzalez-Garcia, Constraining anomalous Higgs interactions, Phys. Rev. D **86**, 075013 (2012).
[22] T. Corbett, O. J. P. Eboli, J. Gonzalez-Fraile, and M. C. Gonzalez-Garcia, Robust determination of the Higgs couplings: Power to the data, Phys. Rev. D **87**, 015022 (2013).
[23] E. Massó and V. Sanz, Limits on anomalous couplings of the Higgs boson to electroweak gauge bosons from LEP and the LHC, Phys. Rev. D **87**, 033001 (2013).
[24] K. Cheung, J. S. Lee, and P. Y. Tseng, Higgs precision (Higgcision) era begins, J. High Energy Phys. 05 (2013) 134.
[25] K. Cheung, J. S. Lee, and P. Y. Tseng, Higgs precision analysis updates 2014, Phys. Rev. D **90**, 095009 (2014).
[26] G. Aad *et al.* (ATLAS and CMS Collaborations), Measurements of the Higgs boson production and decay rates and constraints on its couplings from a combined ATLAS and CMS analysis of the LHC pp collision data at $\sqrt{s} = 7$ and 8 TeV, J. High Energy Phys. 08 (2016) 045.
[27] The ATLAS Collaboration, Measurements of Higgs boson properties in the diphoton decay channel using 80 fb^{-1} of pp collision data at $\sqrt{s} = 13$ TeV with the ATLAS detector, Report No. ATLAS-CONF-2018-028.
[28] A. M. Sirunyan *et al.* (CMS Collaboration), Measurements of Higgs boson properties in the diphoton decay channel in proton-proton collisions at $\sqrt{s} = 13$ TeV, J. High Energy Phys. 11 (2018) 185.
[29] The ATLAS Collaboration, Measurements of the Higgs boson production, fiducial and differential cross sections in the 4ℓ decay channel at $\sqrt{s} = 13$ TeV with the ATLAS detector, Report No. ATLAS-CONF-2018-018.

[30] CMS Collaboration, Measurements of properties of the Higgs boson in the four-lepton final state at $\sqrt{s} = 13$ TeV, Report No. CMS-PAS-HIG-18-001.
[31] The ATLAS Collaboration, Measurement of gluon fusion and vector boson fusion Higgs boson production cross-sections in the $H \to WW^* \to e\nu\mu\nu$ decay channel in pp collisions at $\sqrt{s} = 13$ TeV with the ATLAS detector, Report No. ATLAS-CONF-2018-004.
[32] CMS Collaboration, Measurements of properties of the Higgs boson decaying to a W boson pair in pp collisions at $\sqrt{s} = 13$ TeV, Report No. CMS-PAS-HIG-16-042.
[33] M. Aaboud *et al.* (ATLAS Collaboration), Observation of $H \to b\bar{b}$ decays and VH production with the ATLAS detector, Phys. Lett. B **786**, 59 (2018).
[34] CMS Collaboration, Combined measurements of the Higgs boson's couplings at $\sqrt{s} = 13$ TeV, Report No. CMS-PAS-HIG-17-031.
[35] A. M. Sirunyan *et al.* (CMS Collaboration), Observation of Higgs Boson Decay to Bottom Quarks, Phys. Rev. Lett. **121**, 121801 (2018).
[36] The ATLAS Collaboration, Cross-section measurements of the Higgs boson decaying to a pair of tau leptons in proton–proton collisions at $\sqrt{s} = 13$ TeV with the ATLAS detector, Report No. ATLAS-CONF-2018-021.
[37] CMS Collaboration, Search for the standard model Higgs boson decaying to a pair of τ leptons and produced in association with a W or a Z boson in proton-proton collisions at $\sqrt{s} = 13$ TeV, Report No. CMS-PAS-HIG-18-007.
[38] M. Aaboud *et al.* (ATLAS Collaboration), Observation of Higgs boson production in association with a top quark pair at the LHC with the ATLAS detector, Phys. Lett. B **784**, 173 (2018).
[39] M. Aaboud *et al.* (ATLAS Collaboration), Evidence for the associated production of the Higgs boson and a top quark pair with the ATLAS detector, Phys. Rev. D **97**, 072003 (2018).
[40] M. Aaboud *et al.* (ATLAS Collaboration), Search for the Standard Model Higgs boson produced in association with top quarks and decaying into a $b\bar{b}$ pair in pp collisions at $\sqrt{s} = 13$ TeV with the ATLAS detector, Phys. Rev. D **97**, 072016 (2018).
[41] A. M. Sirunyan *et al.* (CMS Collaboration), Evidence for associated production of a Higgs boson with a top quark pair in final states with electrons, muons, and hadronically decaying τ leptons at $\sqrt{s} = 13$ TeV, J. High Energy Phys. 08 (2018) 066.
[42] A. M. Sirunyan *et al.* (CMS Collaboration), Search for $t\bar{t}H$ production in the all-jet final state in proton-proton collisions at $\sqrt{s} = 13$ TeV, J. High Energy Phys. 06 (2018) 101.
[43] A. M. Sirunyan *et al.* (CMS Collaboration), Search for $t\bar{t}H$ production in the $H \to b\bar{b}$ decay channel with leptonic $t\bar{t}$ decays in proton-proton collisions at $\sqrt{s} = 13$ TeV, J. High Energy Phys. 03 (**2019**) 026.
[44] A. M. Sirunyan *et al.* (CMS Collaboration), Combined measurements of Higgs boson couplings in proton–proton collisions at $\sqrt{s} = 13$ TeV, Eur. Phys. J. C **79**, 421 (2019).
[45] G. Aad *et al.* (ATLAS Collaboration), Combined measurements of Higgs boson production and decay using up to 80 fb^{-1} of proton-proton collision data at $\sqrt{s} = 13$ TeV collected with the ATLAS experiment, Phys. Rev. D **101**, 012002 (2020).
[46] K. Cheung, J. S. Lee, and P. Y. Tseng, New emerging results in higgs precision analysis updates 2018 after establishment of third-generation yukawa couplings, J. High Energy Phys. 09 (**2019**) 098.
[47] (ATLAS Collaboration), A combination of measurements of Higgs boson production and decay using up to 139 fb^{-1} of proton–proton collision data at $\sqrt{s} = 13$ TeV collected with the ATLAS experiment, Report No. ATLAS-CONF-2020-027.
[48] (CMS Collaboration), Combined Higgs boson production and decay measurements with up to 137 fb^{-1} of proton-proton collision data at $\sqrt{s} = 13$ TeV, Report No. CMS-PAS-HIG-19-005.
[49] For a recent review, see, for example, M. Khlopov, What comes after the Standard Model?, Prog. Part. Nucl. Phys. **116**, 103824 (2021).
[50] J. F. Gunion, H. E. Haber, G. L. Kane, and S. Dawson, The Higgs hunter's guide, Front. Phys. **80**, 1 (2000).
[51] J. F. Gunion, H. E. Haber, G. L. Kane, and S. Dawson, Errata for the Higgs hunter's guide, arXiv:hep-ph/9302272.
[52] M. Carena and H. E. Haber, Higgs boson theory and phenomenology, Prog. Part. Nucl. Phys. **50**, 63 (2003).
[53] A. Djouadi, The anatomy of electro-weak symmetry breaking. I: The Higgs boson in the standard model, Phys. Rep. **457**, 1 (2008).
[54] A. Djouadi, The anatomy of electro-weak symmetry breaking. II. The Higgs bosons in the minimal supersymmetric model, Phys. Rep. **459**, 1 (2008).
[55] E. Accomando, A. G. Akeroyd, E. Akhmetzyanova, J. Albert, A. Alves, N. Amapane, M. Aoki, G. Azuelos, S. Baffioni, A. Ballestrero *et al.*, in *Proceeding of the Workshop on CP Studies and Non-Standard Higgs Physics*, 10.5170/CERN-2006-009.
[56] D. Eriksson, J. Rathsman, and O. Stal, 2HDMC: Two-Higgs-doublet model calculator physics and manual, Comput. Phys. Commun. **181**, 189 (2010).
[57] S. Dittmaier *et al.* (LHC Higgs Cross Section Working Group), Handbook of LHC Higgs Cross Sections: 1. Inclusive Observables, 10.5170/CERN-2011-002.
[58] S. Dittmaier, C. Mariotti, G. Passarino, R. Tanaka, S. Alekhin, J. Alwall, E. A. Bagnaschi, A. Banfi, J. Blumlein, S. Bolognesi *et al.*, Handbook of LHC Higgs Cross Sections: 2. Differential Distributions, 10.5170/CERN-2012-002.
[59] S. Heinemeyer *et al.* (LHC Higgs Cross Section Working Group), Handbook of LHC Higgs Cross Sections: 3. Higgs Properties, 10.5170/CERN-2013-004.
[60] D. de Florian *et al.* (LHC Higgs Cross Section Working Group), Handbook of LHC Higgs cross sections: 4. Deciphering the nature of the Higgs sector, arXiv:1610.07922.
[61] S. Dawson, A. Gritsan, H. Logan, J. Qian, C. Tully, R. Van Kooten, A. Ajaib, A. Anastassov, I. Anderson, D. Asner *et al.*, Working group report: Higgs boson, arXiv:1310.8361.
[62] M. Spira, QCD effects in Higgs physics, Fortschr. Phys. **46**, 203 (1998).
[63] M. Spira, Higgs boson production and decay at hadron colliders, Prog. Part. Nucl. Phys. **95**, 98 (2017).

[64] S. Dawson, C. Englert, and T. Plehn, Higgs physics: It ain't over till it's over, Phys. Rep. **816**, 1 (2019).
[65] S. Y. Choi, J. S. Lee, and J. Park, Decays of Higgs bosons in the standard model and beyond, Prog. Part. Nucl. Phys. **120**, 103880 (2021).
[66] T. D. Lee, A theory of spontaneous T violation, Phys. Rev. D **8**, 1226 (1973).
[67] T. D. Lee, CP nonconservation and spontaneous symmetry breaking, Phys. Rep. **9**, 143 (1974).
[68] R. D. Peccei and H. R. Quinn, CP Conservation in the Presence of Instantons, Phys. Rev. Lett. **38**, 1440 (1977).
[69] P. Fayet, A gauge theory of weak and electromagnetic interactions with spontaneous parity breaking, Nucl. Phys. **B78**, 14 (1974).
[70] K. Inoue, A. Kakuto, H. Komatsu, and S. Takeshita, Low-energy parameters and particle masses in a supersymmetric grand unified model, Prog. Theor. Phys. **67**, 1889 (1982).
[71] R. A. Flores and M. Sher, Higgs masses in the standard, multi-Higgs and supersymmetric models, Ann. Phys. (N.Y.) **148**, 95 (1983).
[72] J. F. Gunion and H. E. Haber, Higgs bosons in supersymmetric models. 1., Nucl. Phys. **B272**, 1 (1986); **B402**, 567(E) (1993).
[73] F. J. Botella and J. P. Silva, Jarlskog—like invariants for theories with scalars and fermions, Phys. Rev. D **51**, 3870 (1995).
[74] G. C. Branco, L. Lavoura, and J. P. Silva, CP violation, Int. Ser. Monogr. Phys. **103**, 1 (1999).
[75] G. C. Branco, P. M. Ferreira, L. Lavoura, M. N. Rebelo, M. Sher, and J. P. Silva, Theory and phenomenology of two-Higgs-doublet models, Phys. Rep. **516**, 1 (2012).
[76] A. M. Sirunyan *et al.* (CMS Collaboration), A measurement of the Higgs boson mass in the diphoton decay channel, Phys. Lett. B **805**, 135425 (2020).
[77] H. E. Haber and Y. Nir, Multiscalar models with a high-energy scale, Nucl. Phys. **B335**, 363 (1990).
[78] J. F. Gunion and H. E. Haber, The CP conserving two Higgs doublet model: The approach to the decoupling limit, Phys. Rev. D **67**, 075019 (2003).
[79] N. Craig, J. Galloway, and S. Thomas, Searching for signs of the second Higgs doublet, arXiv:1305.2424.
[80] M. Carena, I. Low, N. R. Shah, and C. E. M. Wagner, Impersonating the standard model Higgs boson: Alignment without decoupling, J. High Energy Phys. 04 (2014) 015.
[81] P. S. Bhupal Dev and A. Pilaftsis, Maximally symmetric two Higgs doublet model with natural standard model alignment, J. High Energy Phys. 12 (2014) 024; 11 (2015) 147(E).
[82] J. Bernon, J. F. Gunion, H. E. Haber, Y. Jiang, and S. Kraml, Scrutinizing the alignment limit in two-Higgs-doublet models: $m_h = 125$ GeV, Phys. Rev. D **92**, 075004 (2015).
[83] M. Carena, H. E. Haber, I. Low, N. R. Shah, and C. E. M. Wagner, Complementarity between nonstandard Higgs boson searches and precision Higgs boson measurements in the MSSM, Phys. Rev. D **91**, 035003 (2015).
[84] B. Grzadkowski, H. E. Haber, O. M. Ogreid, and P. Osland, Heavy Higgs boson decays in the alignment limit of the 2HDM, J. High Energy Phys. 12 (2018) 056.
[85] S. Kanemura, M. Kubota, and K. Yagyu, Aligned CP-violating Higgs sector canceling the electric dipole moment, J. High Energy Phys. 08 (2020) 026.
[86] I. Low, N. R. Shah, and X. P. Wang, Higgs alignment and novel CP-violating observables in 2HDM, Phys. Rev. D **105**, 035009 (2022).
[87] S. P. Li, X. Q. Li, Y. Y. Li, Y. D. Yang, and X. Zhang, Power-aligned 2HDM: A correlative perspective on $(g-2)_{e,\mu}$, J. High Energy Phys. 01 (2021) 034.
[88] J. F. Donoghue and L. F. Li, Properties of charged Higgs bosons, Phys. Rev. D **19**, 945 (1979).
[89] H. Georgi and D. V. Nanopoulos, Suppression of flavor changing effects from neutral spinless meson exchange in gauge theories, Phys. Lett. **82B**, 95 (1979).
[90] S. Davidson and H. E. Haber, Basis-independent methods for the two-Higgs-doublet model, Phys. Rev. D **72**, 035004 (2005); **72**, 099902(E) (2005).
[91] H. E. Haber and D. O'Neil, Basis-independent methods for the two-Higgs-doublet model. II. The significance of $\tan\beta$, Phys. Rev. D **74**, 015018 (2006); **74**, 059905(E) (2006).
[92] R. Boto, T. V. Fernandes, H. E. Haber, J. C. Romão, and J. P. Silva, Basis-independent treatment of the complex 2HDM, Phys. Rev. D **101**, 055023 (2020).
[93] A. V. Manohar and M. B. Wise, Flavor changing neutral currents, an extended scalar sector, and the Higgs production rate at the CERN LHC, Phys. Rev. D **74**, 035009 (2006).
[94] A. Pich and P. Tuzon, Yukawa alignment in the two-Higgs-doublet model, Phys. Rev. D **80**, 091702 (2009).
[95] A. Peñuelas and A. Pich, Flavour alignment in multi-Higgs-doublet models, J. High Energy Phys. 12 (2017) 084.
[96] M. Jung, A. Pich, and P. Tuzon, Charged-Higgs phenomenology in the aligned two-Higgs-doublet model, J. High Energy Phys. 11 (2010) 003.
[97] C. B. Braeuninger, A. Ibarra, and C. Simonetto, Radiatively induced flavour violation in the general two-Higgs doublet model with Yukawa alignment, Phys. Lett. B **692**, 189 (2010).
[98] J. Bijnens, J. Lu, and J. Rathsman, Constraining general two Higgs doublet models by the evolution of Yukawa couplings, J. High Energy Phys. 05 (2012) 118.
[99] P. M. Ferreira, J. F. Gunion, H. E. Haber, and R. Santos, Probing wrong-sign Yukawa couplings at the LHC and a future linear collider, Phys. Rev. D **89**, 115003 (2014).
[100] P. M. Ferreira, R. Guedes, M. O. P. Sampaio, and R. Santos, Wrong sign and symmetric limits and non-decoupling in 2HDMs, J. High Energy Phys. 12 (2014) 067.
[101] A. Biswas and A. Lahiri, Alignment, reverse alignment, and wrong sign Yukawa couplings in two Higgs doublet models, Phys. Rev. D **93**, 115017 (2016).
[102] N. M. Coyle, B. Li, and C. E. M. Wagner, Wrong sign bottom Yukawa coupling in low energy supersymmetry, Phys. Rev. D **97**, 115028 (2018).
[103] D. Egana-Ugrinovic, S. Homiller, and P. R. Meade, Higgs bosons with large couplings to light quarks, Phys. Rev. D **100**, 115041 (2019).
[104] S. L. Glashow and S. Weinberg, Natural conservation laws for neutral currents, Phys. Rev. D **15** (1977) 1958.

[105] K. Cheung, J. S. Lee, and P. Y. Tseng, Higgcision in the two-Higgs doublet models, J. High Energy Phys. 01 (2014) 085.

[106] M. Jung, A. Pich, and P. Tuzon, The $\bar{B} \to X_s\gamma$ rate and CP asymmetry within the aligned two-Higgs-doublet model, Phys. Rev. D **83**, 074011 (2011).

[107] A. Crivellin, A. Kokulu, and C. Greub, Flavor-phenomenology of two-Higgs-doublet models with generic Yukawa structure, Phys. Rev. D **87**, 094031 (2013).

[108] D. Jurčiukonis and L. Lavoura, The three- and four-Higgs couplings in the general two-Higgs-doublet model, J. High Energy Phys. 12 (2018) 004.

[109] S. Kanemura and K. Yagyu, Unitarity bound in the most general two Higgs doublet model, Phys. Lett. B **751**, 289 (2015).

[110] M. E. Peskin and T. Takeuchi, A New Constraint on a Strongly Interacting Higgs Sector, Phys. Rev. Lett. **65**, 964 (1990).

[111] M. E. Peskin and T. Takeuchi, Estimation of oblique electroweak corrections, Phys. Rev. D **46**, 381 (1992).

[112] P. A. Zyla *et al.* (Particle Data Group), Review of particle physics, Prog. Theor. Exp. Phys. **2020**, 083C01 (2020).

[113] D. Toussaint, Renormalization effects from superheavy Higgs particles, Phys. Rev. D **18**, 1626 (1978).

[114] J. S. Lee and A. Pilaftsis, Radiative corrections to scalar masses and mixing in a scale invariant two Higgs doublet model, Phys. Rev. D **86**, 035004 (2012).

[115] S. Kanemura, Y. Okada, H. Taniguchi, and K. Tsumura, Indirect bounds on heavy scalar masses of the two-Higgs-doublet model in light of recent Higgs boson searches, Phys. Lett. B **704**, 303 (2011).

[116] F. Borzumati and C. Greub, 2HDMs predictions for anti-$\bar{B} \to X_s\gamma$ in NLO QCD, Phys. Rev. D **58**, 074004 (1998).

[117] M. Aaboud *et al.* (ATLAS Collaboration), Search for additional heavy neutral Higgs and gauge bosons in the ditau final state produced in 36 fb^{-1} of pp collisions at $\sqrt{s} = 13$ TeV with the ATLAS detector, J. High Energy Phys. 01 (2018) 055.

[118] A. M. Sirunyan *et al.* (CMS Collaboration), Search for additional neutral MSSM Higgs bosons in the $\tau\tau$ final state in proton-proton collisions at $\sqrt{s} = 13$ TeV, J. High Energy Phys. 09 (2018) 007.

[119] A. Bailey (ATLAS and CMS Collaborations), Searches for BSM Higgs bosons at ATLAS and CMS, Proc. Sci. LHCP2020 (**2021**) 011.

[120] G. Aad *et al.* (ATLAS Collaboration), Search for Heavy Higgs Bosons Decaying into Two Tau Leptons with the ATLAS Detector Using pp Collisions at $\sqrt{s} = 13$ TeV, Phys. Rev. Lett. **125**, 051801 (2020).

[121] A. M. Sirunyan *et al.* (CMS Collaboration), Search for beyond the standard model Higgs bosons decaying into a $b\bar{b}$ pair in pp collisions at $\sqrt{s} = 13$ TeV, J. High Energy Phys. 08 (2018) 113.

[122] M. Aaboud *et al.* (ATLAS Collaboration), Search for Heavy Higgs Bosons A/H Decaying to a Top Quark Pair in pp Collisions at $\sqrt{s} = 8$ TeV with the ATLAS Detector, Phys. Rev. Lett. **119**, 191803 (2017).

[123] A. M. Sirunyan *et al.* (CMS Collaboration), Search for production of four top quarks in final states with same-sign or multiple leptons in proton-proton collisions at $\sqrt{s} = 13$ TeV, Eur. Phys. J. C **80**, 75 (2020).

[124] (ATLAS Collaboration), Search for $t\bar{t}H/A \to t\bar{t}t\bar{t}$ production in the multilepton final state in proton-proton collisions at $\sqrt{s} = 13$ TeV with the ATLAS detector, Report No. ATLAS-CONF-2022-008.

[125] M. Aaboud *et al.* (ATLAS Collaboration), Search for WW/WZ resonance production in $\ell\nu qq$ final states in pp collisions at $\sqrt{s} = 13$ TeV with the ATLAS detector, J. High Energy Phys. 03 (**2018**) 042.

[126] M. Aaboud *et al.* (ATLAS Collaboration), Search for heavy ZZ resonances in the $\ell^+\ell^-\ell^+\ell^-$ and $\ell^+\ell^-\nu\bar{\nu}$ final states using proton–proton collisions at $\sqrt{s} = 13$ TeV with the ATLAS detector, Eur. Phys. J. C **78**, 293 (2018).

[127] M. Aaboud *et al.* (ATLAS Collaboration), Searches for heavy ZZ and ZW resonances in the $\ell\ell qq$ and $\nu\nu qq$ final states in pp collisions at $\sqrt{s} = 13$ TeV with the ATLAS detector, J. High Energy Phys. 03 (2018) 009.

[128] A. M. Sirunyan *et al.* (CMS Collaboration), Search for a new scalar resonance decaying to a pair of Z bosons in proton-proton collisions at $\sqrt{s} = 13$ TeV, J. High Energy Phys. 06 (2018) 127; 03 (2019) 128(E).

[129] G. Aad *et al.* (ATLAS Collaboration), Search for heavy resonances decaying into a pair of Z bosons in the $\ell^+\ell^-\ell'^+\ell'^-$ and $\ell^+\ell^-\nu\bar{\nu}$ final states using 139 fb^{-1} of proton–proton collisions at $\sqrt{s} = 13$ TeV with the ATLAS detector, Eur. Phys. J. C **81**, 332 (2021).

[130] M. Aaboud *et al.* (ATLAS Collaboration), Search for heavy resonances decaying into a W or Z boson and a Higgs boson in final states with leptons and b-jets in 36 fb^{-1} of $\sqrt{s} = 13$ TeV pp collisions with the ATLAS detector, J. High Energy Phys. 03 (2018) 174; 11 (2018) 051(E).

[131] A. M. Sirunyan *et al.* (CMS Collaboration), Search for a heavy pseudoscalar boson decaying to a Z and a Higgs boson at $\sqrt{s} = 13$ TeV, Eur. Phys. J. C **79**, 564 (2019).

[132] M. Aaboud *et al.* (ATLAS Collaboration), Search for charged Higgs bosons decaying via $H^\pm \to \tau^\pm\nu_\tau$ in the $\tau +$ jets and $\tau +$ lepton final states with 36 fb^{-1} of pp collision data recorded at $\sqrt{s} = 13$ TeV with the ATLAS experiment, J. High Energy Phys. 09 (2018) 139.

[133] A. M. Sirunyan *et al.* (CMS Collaboration), Search for charged Higgs bosons in the $H^\pm \to \tau^\pm\nu_\tau$ decay channel in proton-proton collisions at $\sqrt{s} = 13$ TeV, J. High Energy Phys. 07 (2019) 142.

[134] M. Aaboud *et al.* (ATLAS Collaboration), Search for charged Higgs bosons decaying into top and bottom quarks at $\sqrt{s} = 13$ TeV with the ATLAS detector, J. High Energy Phys. 11 (2018) 085.

[135] A. M. Sirunyan *et al.* (CMS Collaboration), Search for charged Higgs bosons decaying into a top and a bottom quark in the all-jet final state of pp collisions at $\sqrt{s} = 13$ TeV, J. High Energy Phys. 07 (2020) 126.

[136] G. Aad *et al.* (ATLAS Collaboration), Search for charged Higgs bosons decaying into a top quark and a bottom quark at $\sqrt{s} = 13$ TeV with the ATLAS detector, J. High Energy Phys. 06 (2021) 145.

[137] A. M. Sirunyan *et al.* (CMS Collaboration), Search for a charged Higgs boson decaying to charm and bottom

quarks in proton-proton collisions at $\sqrt{s} = 8$ TeV, J. High Energy Phys. 11 (2018) 115.

[138] V. Khachatryan *et al.* (CMS Collaboration), Search for a light charged Higgs boson decaying to $c\bar{s}$ in pp collisions at $\sqrt{s} = 8$ TeV, J. High Energy Phys. 12 (2015) 178.

[139] A. M. Sirunyan *et al.* (CMS Collaboration), Search for a light charged Higgs boson in the $H^{\pm} \to cs$ channel in proton-proton collisions at $\sqrt{s} = 13$ TeV, Phys. Rev. D **102**, 072001 (2020).

[140] O. Eberhardt, A. P. Martínez, and A. Pich, Global fits in the aligned two-Higgs-doublet model, J. High Energy Phys. 05 (2021) 005.

[141] S. Y. Choi, J. S. Lee, and J. Park, Alignment of Yukawa couplings in two Higgs doublet models, arXiv:2011.04978.